NUREG/IA-0406

International Agreement Report

Post-Test Calculations on Steam Cool-Down Test QUENCH-04 with RELAP5, SCDAP/RELAP5, and TRACE

Prepared by:
Ch. Homann, W. Hering

Karlsruhe Institute of Technology (KIT)
Institute for Neutron Physics and Reactor Technology (INR)
76344 Eggenstein-Leopoldshafen, Germany

A. Calvo, NRC Project Manager

Office of Nuclear Regulatory Research
U.S. Nuclear Regulatory Commission
Washington, DC 20555-0001

Manuscript Completed: July 2011
Date Published: December 2011

Prepared as part of
The Agreement on Research Participation and Technical Exchange
Under the Thermal-Hydraulic Code Applications and Maintenance Program (CAMP)

Published by
U.S. Nuclear Regulatory Commission

AVAILABILITY OF REFERENCE MATERIALS IN NRC PUBLICATIONS

NRC Reference Material

As of November 1999, you may electronically access NUREG-series publications and other NRC records at NRC's Public Electronic Reading Room at http://www.nrc.gov/reading-rm.html. Publicly released records include, to name a few, NUREG-series publications; *Federal Register* notices; applicant, licensee, and vendor documents and correspondence; NRC correspondence and internal memoranda; bulletins and information notices; inspection and investigative reports; licensee event reports; and Commission papers and their attachments.

NRC publications in the NUREG series, NRC regulations, and *Title 10, Energy*, in the Code of *Federal Regulations* may also be purchased from one of these two sources.

1. The Superintendent of Documents
   U.S. Government Printing Office
   Mail Stop SSOP
   Washington, DC 20402–0001
   Internet: bookstore.gpo.gov
   Telephone: 202-512-1800
   Fax: 202-512-2250
2. The National Technical Information Service
   Springfield, VA 22161–0002
   www.ntis.gov
   1–800–553–6847 or, locally, 703–605–6000

A single copy of each NRC draft report for comment is available free, to the extent of supply, upon written request as follows:

Address: Office of the Chief Information Officer,
Reproduction and Distribution
Services Section
U.S. Nuclear Regulatory Commission
Washington, DC 20555-0001
E-mail: DISTRIBUTION@nrc.gov
Facsimile: 301–415–2289

Some publications in the NUREG series that are posted at NRC's Web site address http://www.nrc.gov/reading-rm/doc-collections/nuregs are updated periodically and may differ from the last printed version. Although references to material found on a Web site bear the date the material was accessed, the material available on the date cited may subsequently be removed from the site.

Non-NRC Reference Material

Documents available from public and special technical libraries include all open literature items, such as books, journal articles, and transactions, *Federal Register* notices, Federal and State legislation, and congressional reports. Such documents as theses, dissertations, foreign reports and translations, and non-NRC conference proceedings may be purchased from their sponsoring organization.

Copies of industry codes and standards used in a substantive manner in the NRC regulatory process are maintained at—

The NRC Technical Library
Two White Flint North
11545 Rockville Pike
Rockville, MD 20852–2738

These standards are available in the library for reference use by the public. Codes and standards are usually copyrighted and may be purchased from the originating organization or, if they are American National Standards, from—

American National Standards Institute
11 West 42nd Street
New York, NY 10036–8002
www.ansi.org
212–642–4900

Legally binding regulatory requirements are stated only in laws; NRC regulations; licenses, including technical specifications; or orders, not in NUREG-series publications. The views expressed in contractor-prepared publications in this series are not necessarily those of the NRC.

The NUREG series comprises (1) technical and administrative reports and books prepared by the staff (NUREG–XXXX) or agency contractors (NUREG/CR–XXXX), (2) proceedings of conferences (NUREG/CP–XXXX), (3) reports resulting from international agreements (NUREG/IA–XXXX), (4) brochures (NUREG/BR–XXXX), and (5) compilations of legal decisions and orders of the Commission and Atomic and Safety Licensing Boards and of Directors' decisions under Section 2.206 of NRC's regulations (NUREG–0750).

DISCLAIMER: This report was prepared as an account of work sponsored by an agency of the U.S. Government. Neither the U.S. Government nor any agency thereof, nor any employee, makes any warranty, expressed or implied, or assumes any legal liability or responsibility for any third party's use, or the results of such use, of any information, apparatus, product, or process disclosed in this publication, or represents that its use by such third party would not infringe privately owned rights.

NUREG/IA-0406

Post-Test Calculations on Steam Cool-Down Test QUENCH-04 with RELAP5, SCDAP/RELAP5, and TRACE

Manuscript Completed: July 2011
Date Published: January 2012

Prepared by:
Ch. Homann, W. Hering

Karlsruhe Institute of Technology (KIT)
Institute for Neutron Physics and Reactor Technology (INR)
76344 Eggenstein-Leopoldshafen, Germany

A. Calvo, NRC Project Manager

Prepared for:
Division of Systems Analysis
Office of Nuclear Regulatory Research
U.S. Nuclear Regulatory Commission
Washington, DC 20555-0001

ABSTRACT

In this report, the capabilities of RELAP5, SCDAP/RELAP5, and TRACE to describe oxidation of fuel elements by steam and related hydrogen production are assessed. This work is performed on the background of out-of-pile experiments on the reflood of overheated fuel rod simulators in the QUENCH facility and related numerical investigations at the Karlsruhe Institute of Technology. It is found that oxidation effects play a role even below 1500 K, i.e. for a temperature range that is covered by all of these three codes. The present work relies on the detailed representation of the experimental facility as used for many years for pre- and post-test calculations for the various QUENCH tests with SCDAP/RELAP5. The experimental basis is test QUENCH-04 that consisted mainly of a heat-up and a steam cool-down phase as a relatively simple case, but the present work is also a code to code comparison. As a first step, investigations were concentrated on transients before the reflood phase. Code or modeling errors were identified in both RELAP5 and TRACE that impede reliable predictions for such situations.

FOREWORD

If continuous cooling cannot be maintained in a nuclear reactor due to some unforeseen events, reflood of the dry core as soon as possible is the predominant goal to mitigate the consequences of such abnormal situations. If core temperatures at the start of reflood are already elevated, oxidation of cladding material and related release of hydrogen cannot be neglected. For such situations and for temperatures up to about 1500 K, the capabilities of RELAP5 and TRACE are assessed as part of the contribution of the Karlsruhe Institute of Technology (KIT), formerly Forschungszentrum Karlsruhe (FZK), to the international CAMP (Code Application and Maintenance Program) of the US NRC. In a first step, investigations were concentrated on transients before the reflood phase. During the work, it turned out that emphasis should be put on oxidation effects.

CONTENTS

Page

ABSTRACT iii
FOREWORD v
EXECUTIVE SUMMARY xi
ABBREVIATIONS xiii
1 INTRODUCTION 1
2 EXPERIMENTAL BASIS 3
2.1 QUENCH Facility 3
2.2 Instrumentation 7
2.3 Test Conduct 9
3 COMPUTATIONAL SUPPORT OF QUENCH-04 WITH SCDAP/RELAP5 11
3.1 Modeling of the QUENCH Facility 11
3.2 Results 14
4 CALCULATIONS FOR QUENCH-04 WITH RELAP5 21
4.1 Modeling of the QUENCH Facility 21
4.2 Results 23
5 CALCULATIONS FOR ALTERNATE BUNDLE WITH RELAP5 27
5.1 Modeling of the Alternate Bundle 27
5.2 Results 29
6 CALCULATIONS FOR ALTERNATE BUNDLE WITH TRACE 35
7 CONCLUSIONS 47
8 REFERENCES 49
APPENDIX A OXIDATION MODELS 51

FIGURES

		Page
Figure 1	Main components of the QUENCH facility	4
Figure 2	Main flow paths in the QUENCH facility	5
Figure 3	QUENCH-04 fuel rod simulator bundle (top view)	6
Figure 4	Axial locations for temperature measurement	8
Figure 5	Important test parameters of QUENCH-04	9
Figure 6	Nodalization of the QUENCH facility for calculations with SCDAP/RELAP5	12
Figure 7	Selected measured and calculated (S/R5) results for QUENCH-04 (I)	16
Figure 8	Selected measured and calculated (S/R5) results for QUENCH-04 (II)	17
Figure 9	Measured and calculated (S/R5) axial temperature profiles for QUENCH-04	18
Figure 10	Selected measured and calculated (S/R5) axial profiles for QUENCH-04	19
Figure 11	Calculated (S/R5) axial profiles about local power release in QUENCH-04	20
Figure 12	Calculated axial profiles about local electrical power release in QUENCH-04	22
Figure 13	Selected measured and calculated (R5) results for QUENCH-04	24
Figure 14	Calculated (R5) rod and shroud temperatures for QUENCH-04	25
Figure 15	Calculated (R5) temperature derivatives for QUENCH-04	26
Figure 16	Nodalization of alternate bundle with RELAP5	27
Figure 17	Calculated (R5) temperatures for case B	30
Figure 18	Calculated (R5) temperature derivatives for case B	31
Figure 19	Axial profiles for cases A and B with R5	32
Figure 20	Axial profiles for case B with S/R5 and R5	33
Figure 21	Comparison of case A with TRACE, R5, and S/R5	37
Figure 22	Axial profiles for case A with TRACE and R5	38
Figure 23	Comparison of case B with TRACE, R5, and S/R5	39
Figure 24	Axial profiles for cases A and B with TRACE	40
Figure 25	Comparison of case C with TRACE, R5, and S/R5	41
Figure 26	Axial profiles for cases A and C with TRACE	42
Figure 27	Axial profiles for case B with TRACE and R5	43
Figure 28	Axial profiles for case C with TRACE and R5	44
Figure 29	Radial rod temperature differences at various axial levels	45

TABLES

		Page
Table 1	List of cases, calculated with the various codes	28

EXECUTIVE SUMMARY

If continuous cooling cannot be maintained in a nuclear reactor due to some unforeseen events, reflood of the dry core as soon as possible is the predominant goal to mitigate the consequences of such abnormal situations. If core temperatures at the start of reflood are already elevated, oxidation of cladding material and related release of hydrogen cannot be neglected. For such situations and for temperatures up to about 1500 K, the capabilities of RELAP5 and TRACE are assessed as part of the contribution of the Karlsruhe Institute of Technology (KIT), formerly Forschungszentrum Karlsruhe (FZK), to the international CAMP (Code Application and Maintenance Program) of the US NRC. In a first step, investigations were concentrated on transients before the reflood phase. During the work, it turned out that emphasis should be put on oxidation effects.

To rely on a scenario that is prototypical for nuclear reactors, test QUENCH-04 out of a series of out-of-pile bundle experiments, performed at former Forschungszentrum Karlsruhe (FZK), now part of KIT, was used as a basis. In that test, a 21-rod bundle was heated up electrically and cooled down with steam, when a predefined temperature was reached. The input deck for RELAP5 relies on the detailed representation of the experimental facility as used for many years for pre- and post-test calculations for the various QUENCH tests with SCDAP/RELAP5. The post-test calculations with RELAP5 show an unphysical sudden temperature increase of about 50 K during the heat-up phase, leading to subsequent code failure. This is in contrast to respective calculations with SCDAP/RELAP5.

To tackle that problem, the relevant parts were identified and extracted from the original input deck to simplify error tracking. Similar temperature steps as for the original case are calculated with RELAP5, if and only if the oxidation model is activated, whereas no problem exists for SCDAP/RELAP5.

This modified input deck was transformed with SNAP for TRACE calculations to test this follow-up program of RELAP5. The error of RELAP5 calculations did not occur with TRACE, but oxidation heat release is severely underestimated in TRACE, leading to unrealistic results. Some other shortcomings of RELAP5, TRACE, and SNAP are also identified.

It is emphasized that the purpose of the present report is to assess the capabilities of RELAP5 and TRACE and not mainly to present post-test calculations of a given experiment. Among other reasons, the test QUENCH-04 is chosen as an experimental basis to be sure that the chosen scenario is reasonable with respect to reactor safety considerations. Though the agreement between the SCDAP/RELAP5 calculations might be improved, the computational results may well serve as a basis for the present investigations. The outcome of the assessment does not depend on the imperfections mentioned above.

For the various codes and cases, CPU time was below three minutes for about 2000 s of problem time.

ABBREVIATIONS

CAMP	Code Application and Maintenance Program of the US NRC
INR	Institute for Neutron Physics and Reactor Technology at KIT
KIT	Institute of Technology
LOCA	Loss of Coolant Accident
MS	Mass Spectrometer
P_{el}	Total electrical power as derived from measured current and voltage
PWR	Pressurized Water Reactor
R5	RELAP5
RELAP	old: Reactor Excursions and Leak Analysis Program now: Reactor Leak and Analysis Program
S/R5	SCDAP/RELAP5
SCDAP	Severe Core Damage Analysis Package
TC	Thermocouple
TCI	Thermocouple embedded in the inner cooling jacket
TCR	Thermocouple at the central rod outer surface
TCRC	Thermocouple at the central rod centerline
TCRI	Thermocouple at the central rod cladding inner surface
TFS	Thermocouple at the fuel rod simulator (heated rod) outer surface
TIT	Thermocouple at the corner rod centerline
TSH	Thermocouple at the shroud outer wall surface
TRAC	Transient Reactor Analysis Code
TRACE	TRAC/RELAP Advanced Computational Engine
US NRC	United States Nuclear Regulatory Commission

1 INTRODUCTION

If continuous cooling cannot be maintained in a water-cooled nuclear reactor, the core boils down and the structures, above all the fuel rods, heat up. Such a situation may occur, when the station supply power is not available and auxiliary systems fail to start or when a sufficiently large leak occurs and the water, collected in the reactor sump, cannot be used for cooling. Reflood of the dry core as soon as possible is the predominant goal to mitigate the consequences of such abnormal situations. Part of the incoming water boils due to the high temperatures, and the resulting steam reacts chemically with the structures, i.e. above all the cladding material is oxidized, and hydrogen is released. Since oxidation is an exothermic reaction, temperature increases locally. At higher temperatures, these effects cannot be neglected, and this does not only concern design extension, but also design basis conditions.

Computational work for design basis conditions can be done with the US NRC codes RELAP5 [1] and, as a more recent development, TRACE [2], whereas SCDAP/RELAP5 [3] should be used for beyond design basis conditions, because this code also considers material behavior that plays an important role in such situations. All three codes include models for the oxidation of Zircaloy, in the RELAP5 and TRACE manuals called metal-water reaction. The models describe the effects at different levels and with different sophistication, see Appendix A. Though many applications of RELAP5 and TRACE concern lower temperatures, it should be guaranteed that the codes give reliable results in the whole range of applications for which they are intended, i.e. to about 1500 K. Such applications may also be interesting, when new cladding materials are considered.

For this reason, it is the aim of the present work to assess the capabilities of RELAP5 and TRACE for such situations. In a first step, work concentrates on the heat-up phase before reflood initiation to avoid too many problems at a time. In addition, it should be guaranteed that the chosen scenario is prototypical for reactor conditions. Therefore and to enable a respective comparison, the present work is based on an experimental basis.

According to the institute's research focus and the authors' experience about delayed flooding of nuclear reactors, the QUENCH program is used as a basis for the present work. It has been set up at the former Forschungszentrum Karlsruhe (now part of KIT) in the 1990s to study hydrogen generation of an overheated core during water reflood and steam cool-down. In particular, physico-chemical behavior of overheated fuel elements, material interactions at high temperatures, i.e. for design extension conditions are investigated, and a database for model development and code validation is created. On the experimental side, the program consists of separate effects tests and bundle tests. The experimental program now also includes LOCA (Loss of Coolant Accident) conditions with new cladding materials.

For many years, the authors were involved in that program with computational and other analytical work for the bundle tests, starting with the authors' support to construct the related QUENCH facility [04] and continuing with pre- and post-test analysis of many tests. For the calculations on QUENCH tests, mostly the in-house version of SCDAP/RELAP5 mod 3.2 was used, containing models for special features of the QUENCH facility [5]; code version mod 3.3 was seen to be inoperable for the QUENCH tests.

Since the assessment of RELAP5 and TRACE for pre-reflood conditions, aim and subject of the present report, should be done on a simple basis, test QUENCH-04 [6] has been chosen out of

the 15 bundle tests, run up to now. Related SCDAP/RELAP5 calculations were done with the in-house version [5] of SCDAP/RELAP5 mod 3.2hx shortly after the test. Further changes of the input deck to improve the agreement with experimental data, based on present knowledge of the test facility and the tests, might be possible but could not be done for time reasons. In addition, the deviation between measured and calculated results does not play a critical role in this report: the aim of the present report is to assess the capabilities of RELAP5 and TRACE. This is partly done on an experimental basis, partly as a code to code comparison. In any case, the experiment serves as a guideline that demonstrates that the scenario is by far not a mere academic problem.

In a second step, an input deck for RELAP5 mod 3.3gl was developed out of the SCDAP/RELAP5 input deck and tested. Though the US NRC does not support code development for RELAP5 any longer, the US NRC provides a continued support, including the correction of errors as far as possible, and distributes the code to external partners all aver the world. Therefore, an assessment of its capabilities is still useful. Besides, the RELAP5 input deck could also be used with SCDAP/RELAP5 for comparison, after some small changes were made. In addition, SNAP [7] could be used to convert the RELAP5 input deck for TRACE. This was faster, easier, and more reliable than to develop an input deck by hand. An assessment of that code was therefore done as a final step, using TRACE v5.0p1. This work is even more important than the assessment of RELAP5, because TRACE is under current development, and its use is emphasized by the US NRC.

During the investigations, reported here, it turned out that emphasis should be put on oxidation effects. In contrast to SCDAP/RELAP5 applications, results of RELAP5 and TRACE should only be considered for design basis conditions, and temperatures above about 1500 K in the test should not be considered. Results for higher temperatures are, however, included in the present report because of the chosen experimental basis.

2 EXPERIMENTAL BASIS

2.1 QUENCH Facility

In the following, a short description of various aspects of the QUENCH facility is given with figures taken from [6] and from similar documentation. More details are documented in [6]. The QUENCH facility (see Figure 1), consists of the test section as its main part and a number of external devices (Figure 2). The facility has undergone several modifications during time. The fast water injection has been installed before the conduct of test QUENCH-06 to accelerate flooding of the structures below the bundle for water quenching.

The test section consists of a bundle with 21 rods (Figure 3). Their arrangement and their cladding (Zircaloy-4) are typical for commercial Western type PWRs. The empty space in the rods is filled with a mixture of argon and krypton with some overpressure; the krypton additive allows detecting rod failure during the test with the mass spectrometer. The central rod is unheated; the other 20 rods are fuel rod simulators with annular ZrO_2 pellets. They are heated electrically over a length of 1024 mm; the tungsten heaters are connected to a combination of molybdenum and copper electrodes at both ends. Electrical power supply is independent for the eight inner and the twelve outer fuel rod simulators. The four Zircaloy corner rods (rods with a diameter of 6 mm in Figure 3) are intended to reduce the flow cross section in that region to values that are closer to the normal subchannel size. In this way, they give a flat lateral temperature profile in the bundle and a flat lateral velocity profile during the reflood phase. In addition, the corner rods are used for instrumentation. One or two of them may be removed during the test to analyze the axial profile of the oxide layer thickness, formed up to that time. The rods are held in their positions by five grid spacers; the lowermost grid spacer is made of Inconel, the others of Zircaloy. Their lower edge is at axial positions –200 mm, at 50, 550, 1050, and 1450 mm, respectively, where axial elevation 0 mm is set to the lower end of the heated length.

A mixture of steam and argon enters the bundle from the bottom; the fluid, i.e. steam, argon, hydrogen, leaves the bundle at its top to enter the off-gas pipe. System pressure is set during the starting procedure for a test to about 0.2 MPa by adjusting a spring at a valve near the downstream end of the condenser and upstream of the Caldos instrument for hydrogen detection (Figure 1). There is no control to maintain that value during the test so that the system pressure changes during cool-down by about 0.03 MPa.

The bundle is contained in a Zircaloy shroud. The shroud material contributes to local heating in the hot zone due to oxidation at its inner surface and in this way simulates contributions of the outer parts of a large reactor fuel element and in this way leads to a flatter radial temperature profile in the bundle than with a non-oxidizing shroud material. The bundle and the shroud are insulated by ZrO_2 fiber material in the lower electrode zone and in the heated zone, filling the annulus between shroud and the inner cooling jacket. In the upper electrode zone, there is no insulation to avoid too high temperatures that might damage the electrode material. The bundle and its insulation are cooled by counter-current water (upper electrode zone) and argon (heated zone and lower electrode zone) flows within the cooling jackets. The whole set-up is enclosed in a steel containment for safety reasons.

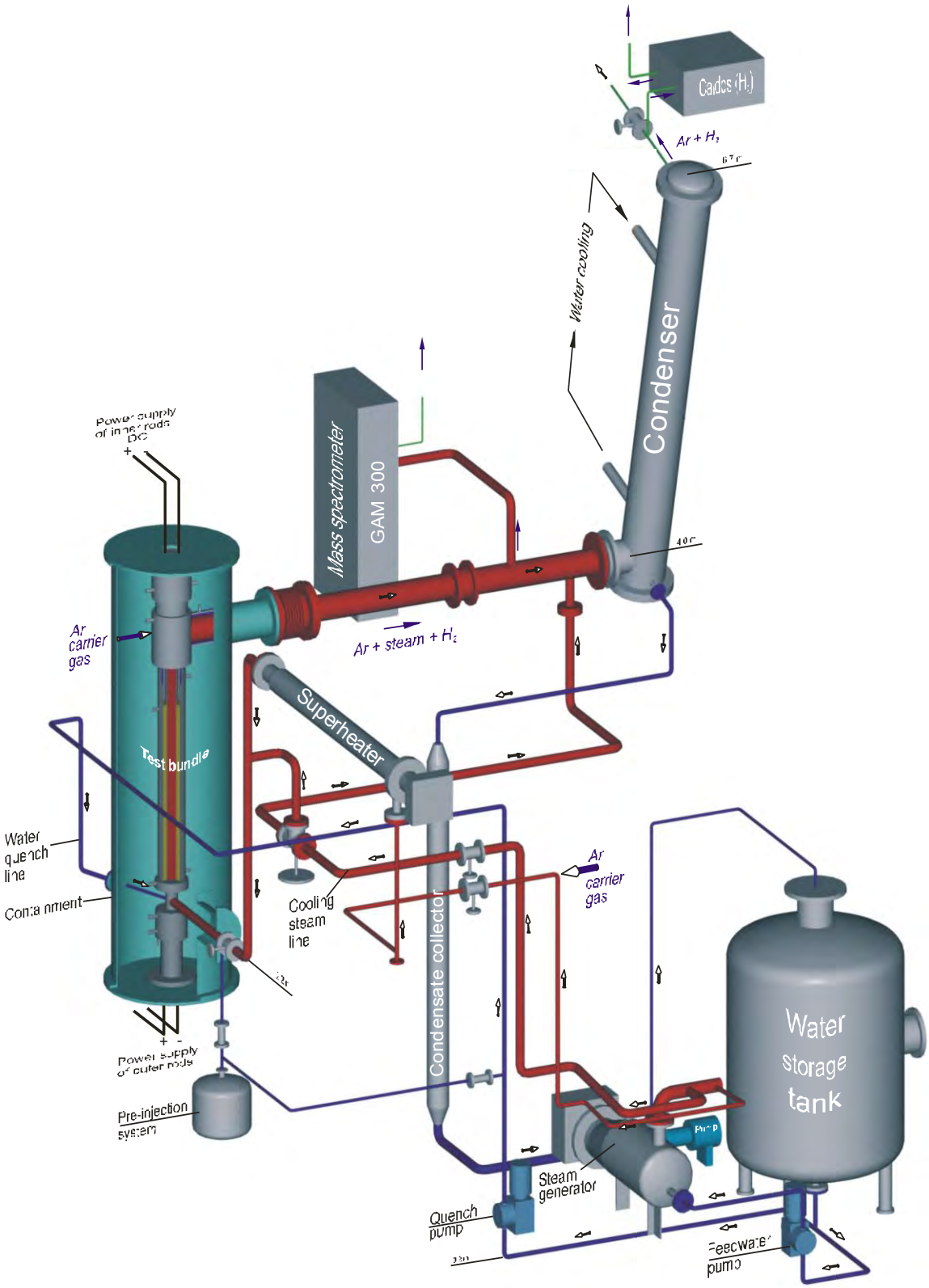

Figure 1 Main components of the QUENCH facility

Fig.2-QUE08-Gesamtanlage.cdr

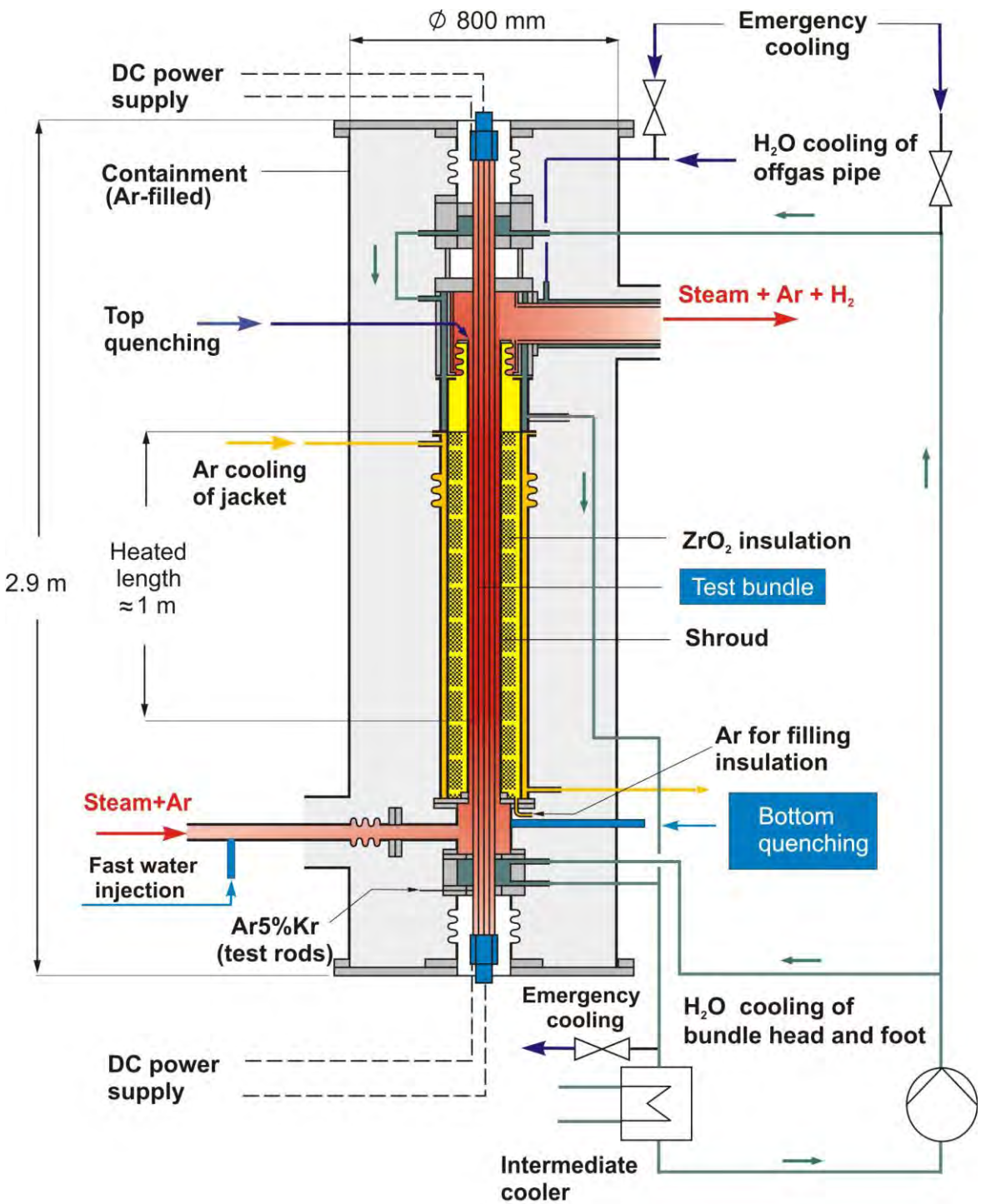

Figure 2 Main flow paths in the QUENCH facility

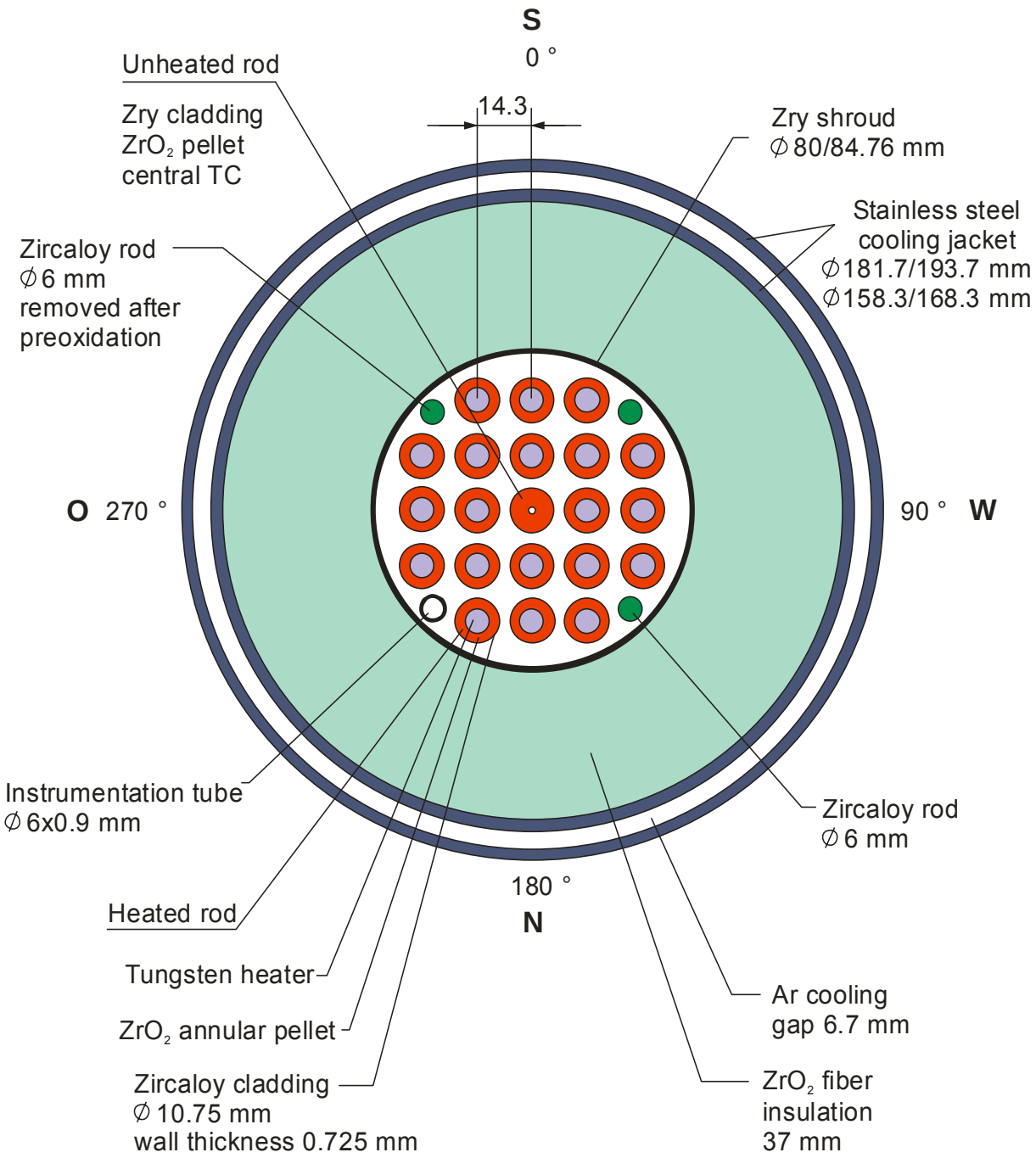

Figure 3 QUENCH-04 fuel rod simulator bundle (top view)

2.2 Instrumentation

The test section is equipped with more than 90 thermocouples at 17 axial locations in the heated and in both electrode zones. The lowest axial position is at –250 mm (level 1); their axial distance from one another is 100 mm. Therefore, levels 4 to 13 refer to instrumentation of the heated zone. TFS and TIT (see list of abbreviations) are TCs on the outer clad surface of fuel rod simulators, and in the centerline of corner rods, respectively. TCRC refers to the central rod centerline, TCRI to the central rod cladding inner surface, and TCR to the central rod cladding outer surface. TCs of type TSH are mounted on the outer shroud surface; TCI are imbedded in the inner cooling jacket. For a given TC, the designation contains the axial level and the radial or azimuthal position. In particular, the designation for TFS is given as i/j, where I refers to the radial position with i=1 for the central rod, i=2 and i=3 for the inner and i=4 and i=5 for the outer heated rods; j indicates the axial level according to Figure 4. More details are given in [6]. At high temperature, it may happen that a TFS or TSH looses its contact with the adjacent surface or that a new TC junction forms due to melting. In such cases, readings become unreliable, and only qualitative conclusions can be drawn, if at all. In the figures of this report, such TCs are not shown after they became unreliable.

The total electrical power P_{el} is calculated as the product of measured current and voltage and summed over the two electrical circuits. Voltage measurement is outside the heated rods and contains voltage drops e.g. in wires and in the sliding contacts at the ends of the heated rods. Therefore, the electrical power, released into the bundle, is smaller than the total electrical power P_{el}. In recent QUENCH tests, the electrical resistance of the sliding contacts has been derived from pre-test measurements of the electrical resistance of the rods. The results indicate that the electrical resistance may vary from test to test. In later tests, related resistances were measured, before the test was performed.

Fluid composition is mainly analyzed by a quadrupole mass spectrometer “GAM 300” at about 2.7 m into the off-gas pipe. Downstream of the condenser, a hydrogen detection system “Caldos 7 G”, based on measuring thermal conductivity of the fluid, and a mass spectrometer “Prisma”, simpler than “GAM 300”, are installed close to each other.

For the GAM 300 MS, several improvements have been made since the start of the QUENCH program [8]. In QUENCH-04, however, measurement of steam mass flow was calibrated with an external source for the QUENCH tests. A pump to decouple the driving pressure drop for the MS from pressure in the off-gas pipe was not yet installed neither. When a large portion of steam is consumed in the bundle, less steam can be condensed in the condenser, and the pressure drop in the condenser should decrease. Due to the argon flow, there is, however, always a residual pressure drop. Since the system pressure is not kept constant at that level during the whole test in one or another way, the original set-up may give unsatisfactory results, especially during cool-down.

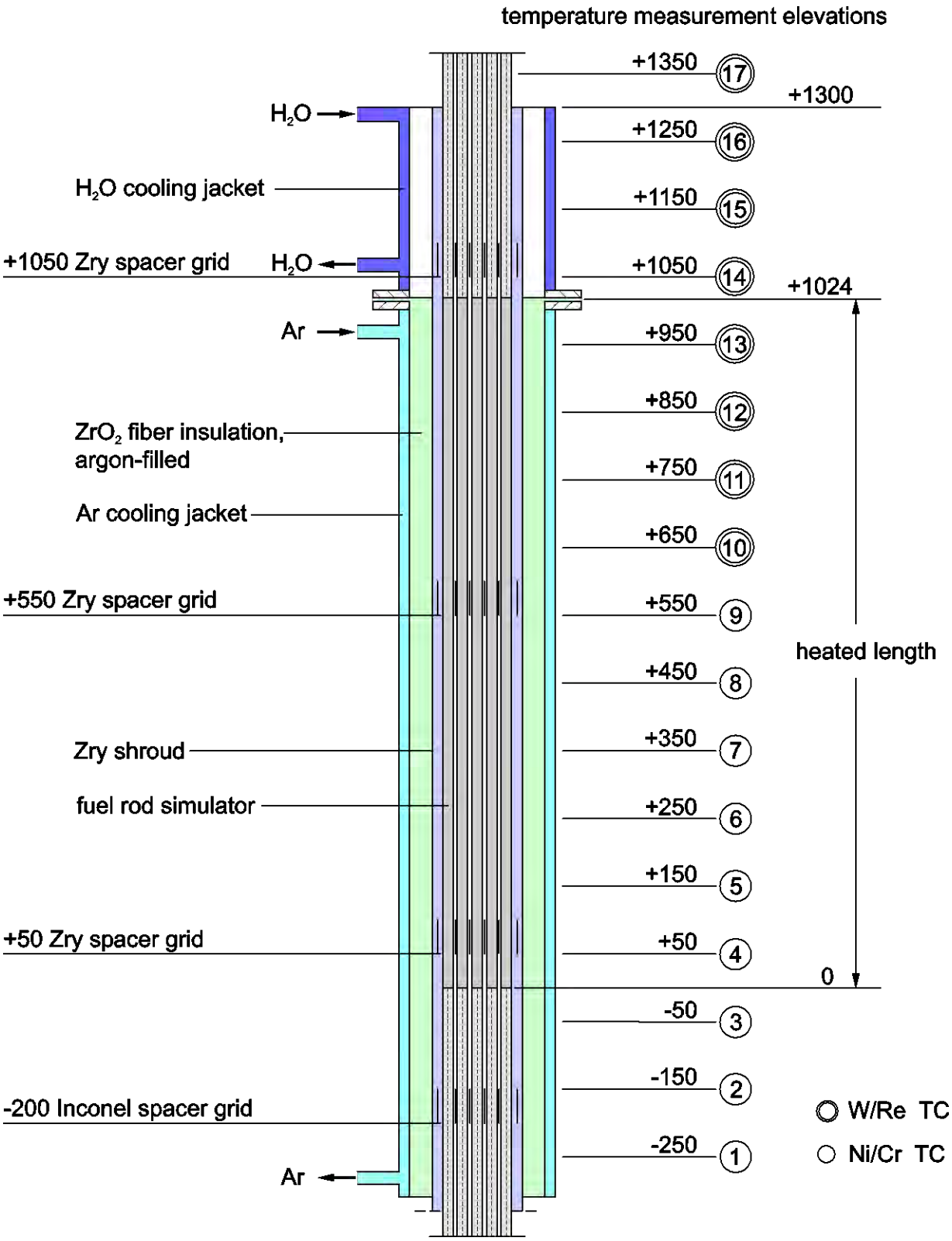

Figure 4 Axial locations for temperature measurement

2.3 Test Conduct

The bundle was heated from room temperature to ~900 K in an atmosphere of flowing argon and steam with 3 g/s each. The bundle was stabilized at this temperature for about 2 hours with an electrical power of 4.3 kW (see Figure 5). At the end of the stabilization period, 121 s after starting data acquisition, the electrical power was increased nearly linearly to a maximum of 16.2 kW so that the bundle was ramped at 0.31 W/s per rod. It resulted in an average temperature increase of about 0.35 K/s between 900 K and 1400 K and of 1.0 K/s between 1400 K and 1750 K. Corner rod B was withdrawn from the bundle at about 2012 s at a maximum bundle temperature of about 1780 K to check the oxide layer thickness accumulated up to that time. The steam cool-down sequence was initiated at a maximum bundle temperature of about 2160 K. The steam flow was turned off at around 2064 s, whereas the argon gas remained unchanged. For cooling the test bundle, steam was injected at the bottom of the test section at a mean rate of 50 g/s for 242 s. At 2088 s, the electrical power was reduced to 4 kW within 15 s, and was shut off at 2302 s. 1 s later, the cool-down steam was turned off, terminating the experiment.

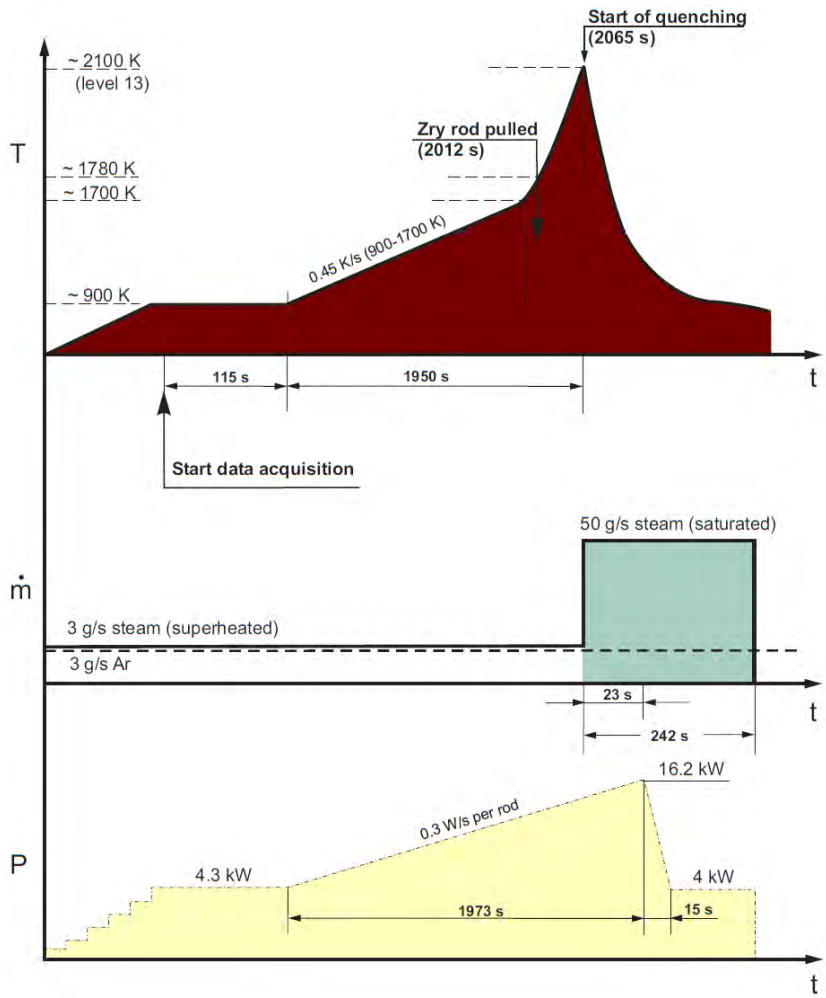

Figure 5 Important test parameters of QUENCH-04

The figure shows from top to bottom a typical temperature at level 13, normally the hottest axial measuring position, bundle inlet mass flow rate, and total electrical power.

3 COMPUTATIONAL SUPPORT OF QUENCH-04 WITH SCDAP/RELAP5

Within KIT/INR R&D activities, calculations have been made to define experimental parameters of the QUENCH experiments up to and including QUENCH-11 and to interpret the experimental results, after the experiment had been performed. For the calculations, the in-house version [5] of SCDAP/RELAP5 mod 3.2 [3] has been used. This code version contains an improved model for heat transfer in the transition-boiling region [9], an adaptation of the SCDAP model for electrically heated fuel rod simulators to the conditions of the QUENCH facility, and the material property data for ZrO_2 instead of those for UO_2 to model the pellets.

The various calculations also rely on the experience gained from calculations, done up to then. With experience, gained afterwards, some changes would be made in the modeling of the facility and test QUENCH-04, and the agreement between experimental and calculated results would probably be improved. However, an improvement of earlier post-test calculations is not the aim of the present investigations. The deviations between experimental and calculated data do not play a critical role in this report; they should therefore not be taken too seriously. In the context of the present report, the test QUENCH-04 is meant as a prototypical example of core heat-up after dry-out and subsequent steam cool-down. In this section, the test is also used to demonstrate the various processes during the test.

3.1 Modeling of the QUENCH Facility

The nodalization scheme of the QUENCH facility is shown in Figure 6. Apart from limited changes and an axial mesh refinement, used in later QUENCH tests, it is the same for all QUENCH tests. In the radial direction, the whole facility including the containment is modeled, because the only reliable boundary condition to calculate the radial heat losses out of the bundle is the ambient room temperature. This concept is mandatory for all work performed before experimental data are available, and it is desirable for all post-test analyses, because the calculated data are more detailed than the experimental ones.

At the time, when calculations for QUENCH-04 were made at INR, the number of axial meshes in SCDAP/RELAP5 was restricted to 16. Axially, the heated part is therefore modeled with ten 0.1 m long meshes. The lower and upper electrode zones are discretized with three meshes each, assuming molybdenum as electrode material. The unheated rod and the four Zircaloy corner rods are modeled as SCDAP fuel rod components and the two rows of rods to be heated independently as SCDAP simulator components. The temperature at the end of the rods is set to 300 K. The shroud, the insulation, the inner and outer cooling jacket, and the containment are modeled as SCDAP shroud components, the shroud, the ZrO_2 insulation, and the inner cooling jacket forming a single component. By using SCDAP components for the facility model, two-dimensional heat conduction within the structures and radiation between adjacent structures are taken into account.

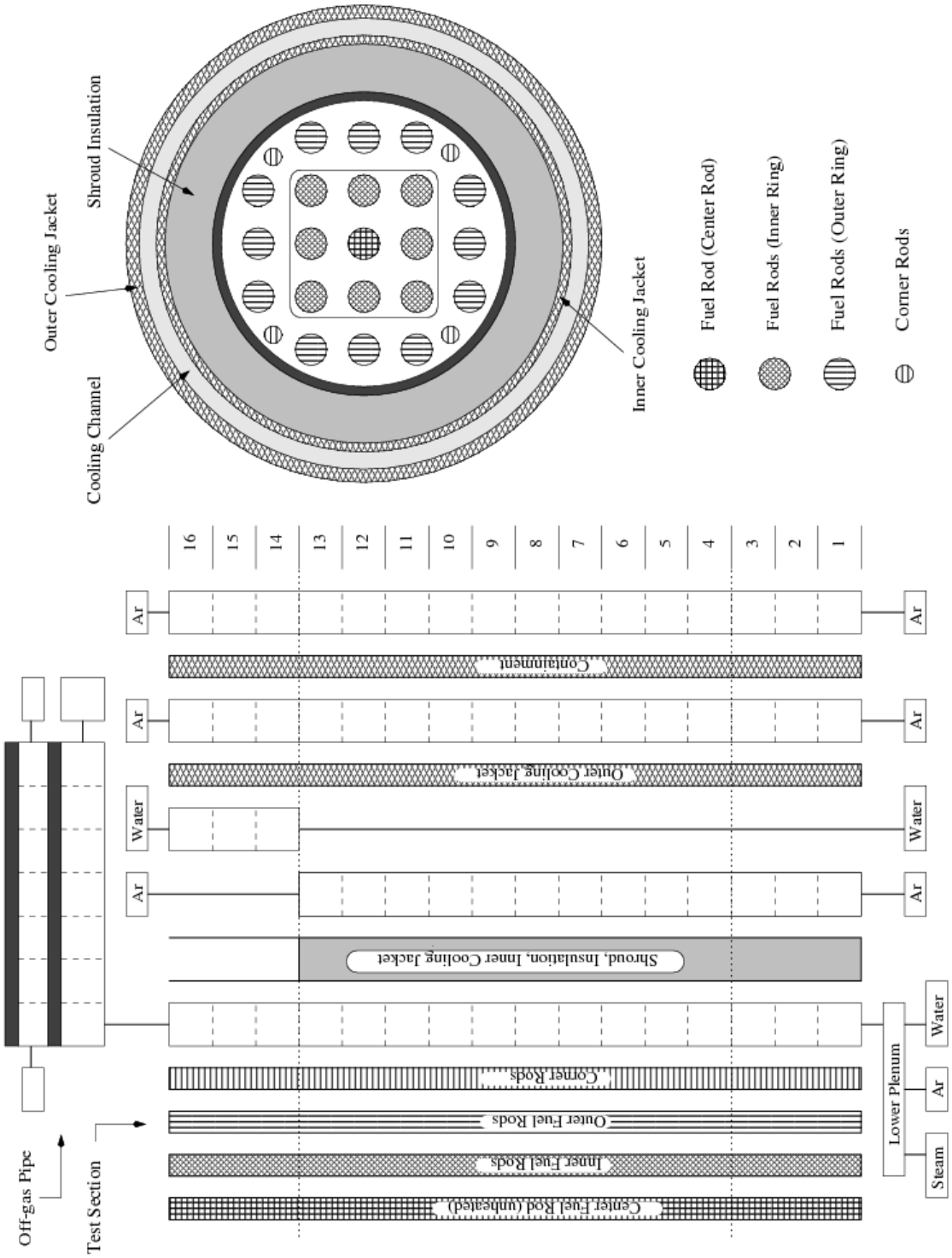

Figure 6 Nodalization of the QUENCH facility for calculations with SCDAP/RELAP5

The ZrO_2 fiber insulation is modeled by code changes to end at the upper end of the heated

zone [5], as it corresponds to the experimental conditions. With this exception, all structures must be modeled to have the same length because of limitations in the code. Therefore, the upper and lower head cannot be modeled in all details. In early stages of INR computational support, it was judged that the correct modeling of geometry of the shroud and the shroud insulation is predominant. This has a drawback on modeling of electrical power input, as will be outlined later.

Due to modeling restrictions in SCDAP/RELAP5, the structures outside the bundle must be represented in Cartesian instead of cylindrical geometry. This approximation is justified, when the thickness of the component is small in comparison to its inner radius. For the first SCDAP component “shroud”, which contains the shroud itself, the shroud insulation and the inner cooling jacket, this assumption is not justified. Therefore, its volume is about 40 % larger than for a Cartesian geometry, and for the same temperature difference, the average heat flux is also larger by about 40 %. Since the major part of this domain is filled by the insulation material, both its specific heat capacity and the thermal conductivity have been increased by 40 % to compensate for this geometry effect. This treatment is, however, only an approximation, because average values for the whole domain are considered, and for a better representation, the use of cylindrical co-ordinates to solve the heat conduction equation is mandatory. For this reason and for a better match with experimental data, heat conduction in the ZrO_2 fiber insulation was adjusted during the post-test calculations for QUENCH-01, and this adjustment has not been changed since, though there is meanwhile information that this modeling might be improved.

For the electrical power history, the experimental information is used directly. The electrical power, released outside the bundle, but inside the region that is included by voltage measurement, is accounted for by a constant electrical resistance outside the bundle [5]. In the calculations, the same value of 4.2 mΩ per rod was used as for post-test calculations for test QUENCH-01 [10].

The bundle flow and the gas atmospheres outside the outer cooling jacket, i.e. in the containment and the laboratory, are represented by a single channel each. The gas atmospheres outside the outer cooling jacket are assumed to be stagnant, thus neglecting natural convection in these regions. Since only a limited number of materials can be specified, these atmospheres are modeled to consist of argon instead of air.

The off-gas pipe is taken into account with its whole length of 3 m, including the orifice at the position where the gas sample for the mass spectrometer is taken and the orifice at the outlet of the off-gas pipe. The mass flows in the off-gas pipe and the adjacent cooling jacket are modeled to be one-dimensional, the structures are modeled as RELAP5 heat structures, thus taking into account radial heat transfer within the structures.

For post-test calculations, fluid inlet temperature has to be adjusted according to the reading of thermocouple TFS 2/1 at –250 mm. This TC is bent into the flow channel to measure the fluid temperature near the bundle inlet. Other information base would be measured fluid temperature T 511 in the inlet pipe, but firstly, this is a local value, not representative for the bulk temperature in that cross section; secondly, heat losses between that TC location and the bundle inlet cannot be neglected. Other input values like mass flow rates and power history are of course taken directly from the experiment. More details of the modeling are discussed in [10].

3.2 Results

Measured and calculated results are given in Figure 7. To give an overview of test QUENCH-04, several graphs are combined in this and in the following figures. The two curves for electrical power (top of the figure) in this and subsequent figures refer to power, released in the bundle, and total electrical power P_{el}, measured in the facility (see sections 2.2 and 3.1 for the difference between them). According to the calculation, 68 % of the total electrical power is released into the bundle at the start of the test and 77 % before decreasing the electrical power at 2088 s. The difference between total electrical power and power, released into the bundle, will play a role throughout the whole investigation. The figure also shows that the released chemical power cannot be neglected with respect to the electrical power input later in the test.

Designations cld2_xx and cld3_xx for the measured temperatures in Figure 7 and subsequent figures refer to calculated results for the inner and outer heated rods, respectively, at axial level xx. The large number of measured values is meant to give an idea of experimental variations and scatter. Calculated results are shown as solid lines in this report. They agree quite well with measured ones in the center of the bundle. They are overestimated at the bottom of the heated length and underestimated at the top of the heated length. These two deviations are related with one another, because the total electrical power input is specified and the local contributions of electrical power release must sum up to the total value. The difference increases with time because of increasing oxidation of Zircaloy claddings and shroud.

These deviations demonstrate a crucial drawback of electrical bundle heating: the electrical resistance of metal heaters increases with temperature. This effect results in an increase of local release of electrical power. Oxidation of the Zircaloy cladding and shroud is exothermic and increases significantly with temperature (top of Figure 7). Both effects are a positive feedback for temperature development in the bundle. The feedback increases with temperature and makes calculations difficult. Things become even worse, when oxidation kinetics change at about 1800 K [11] to even more violent oxidation, leading to temperature escalations, i.e. to fast and strong temperature increases that cannot be compensated by cooling.

In addition, Figure 7 shows that even for temperatures below 1500 K, chemical power release and hence oxidation effects cannot be neglected. This result emphasizes the relevance of the present investigation. Since the effects are underestimated with SCDAP/RELAP5, they are even larger in the test, hence in reality.

Because of underestimated bundle temperatures in the hot zone and the positive feedback, hydrogen production becomes more and more underestimated (Figure 8). The figure also shows that temperatures at the uppermost two axial levels and hence oxide scales are calculated to be nearly the same.

Axial temperature profiles are rather flat in the nearly unheated electrode zones (Figure 9). The decrease in the upper electrode zone is due to the large radial heat losses, because bundle insulation ends at the upper end of the heated zone. If the upper electrode zone were insulated, rod temperatures would become excessively high, and the electrodes would melt, as respective calculations in the construction phase of the facility show [4]. At 0.55 m, the measured bundle and shroud temperatures are somewhat lower than might be expected. This is probably due to a spacer grid at that elevation: local redistribution of the fluid near the spacer grid causes enhanced cooling. The fluid outlet temperature is only given as a rough estimate. Since the respective TC was situated outside the bundle cross section, its reading was influenced by the

radial temperature decrease between the bundle and the water-cooled upper plenum wall and was hence not representative for the bulk values calculated in SCDAP/RELAP5. The figure also gives an impression of the radial temperature profile in the bundle. In addition, it shows the efficiency of argon- and water-cooling outside of the bundle. In spite of the relatively low temperature, radiation between the outer cooling jacket and the containment cannot be neglected, as can be demonstrated with appropriate calculations.

The comparison with measured data shows that calculated axial temperature profiles at the start of the power transient are correct. Later in the transient, the measured high temperatures at the upper end of the heated zone are underestimated. One reason for the deviation is the large axial mesh length that has been reduced in calculations for later tests. The TCs around the upper end of the heated zone that are unreliable at high temperatures in the first QUENCH tests for technical reasons [12] are omitted in Figure 9 for t = 2063 s.

Axial profiles at the time when a corner rod was withdrawn from the bundle are shown in Figure 10. In this and in the subsequent axial plots, the extension of the heated zone is indicated by vertical dotted lines. The calculated oxide scales are quite close together according to the flat radial temperature profile. Since the calculated temperatures in the hot zone are nearly always below the measured ones and since formation of the oxide scale is a cumulative effect that increases with temperature, the oxide scale in the hot zone is clearly underestimated. In contrast to the high temperature region, oxidation is overestimated in the colder parts of the bundle. Therefore, the measured profile of oxide scale is narrower than the calculated one. Oxidation modeling might be improved in principle for such situations, but in severe accident sequences, as addressed in codes like SCDAP/RELAP5, contributions of oxidation at low temperatures to the total hydrogen release are negligible. As an overall result, the figure shows that the hot zone in the bundle is rather limited.

A deeper insight into the various results can be obtained from axial profiles for electrical and chemical power release for various axial temperature profiles (Figure 11). The stepwise initial temperature profile is due to respective approximations in the input deck. In the heated zone, local electrical power release is nearly constant in early times of the test. Later on, the positive feedback due to the metal heater results in higher release of electrical power in the hot zone, and the axial profiles become steeper. Electrical power release in the electrode zones is small due to the electrode material. In contrast, chemical power release occurs dominantly in the small zone around the axial level, where temperature reaches its maximum value, because the increase of oxidation and the related increase of chemical power with temperature are strong. This difference is essential for a correct understanding of such tests and explains the narrow curve for oxidation scale in Figure 10. The different axial profiles of electrical and chemical power release should also be kept in mind, when global values for power release are interpreted as in the top of Figure 7.

The ratio of local chemical to electrical power release clearly demonstrates the role of oxidation. The related chemical power release is spatially limited, but it cannot be neglected above about 1200 K for the current transient. Since the oxidation rate also depends on the current oxide layer thickness, the limit might be lower for faster transients and higher for slower ones. That means that it also concerns the range of design basis conditions. A reliable model is therefore indispensible, and an assessment of the respective capabilities of codes like RELAP5 and TRACE is justified.

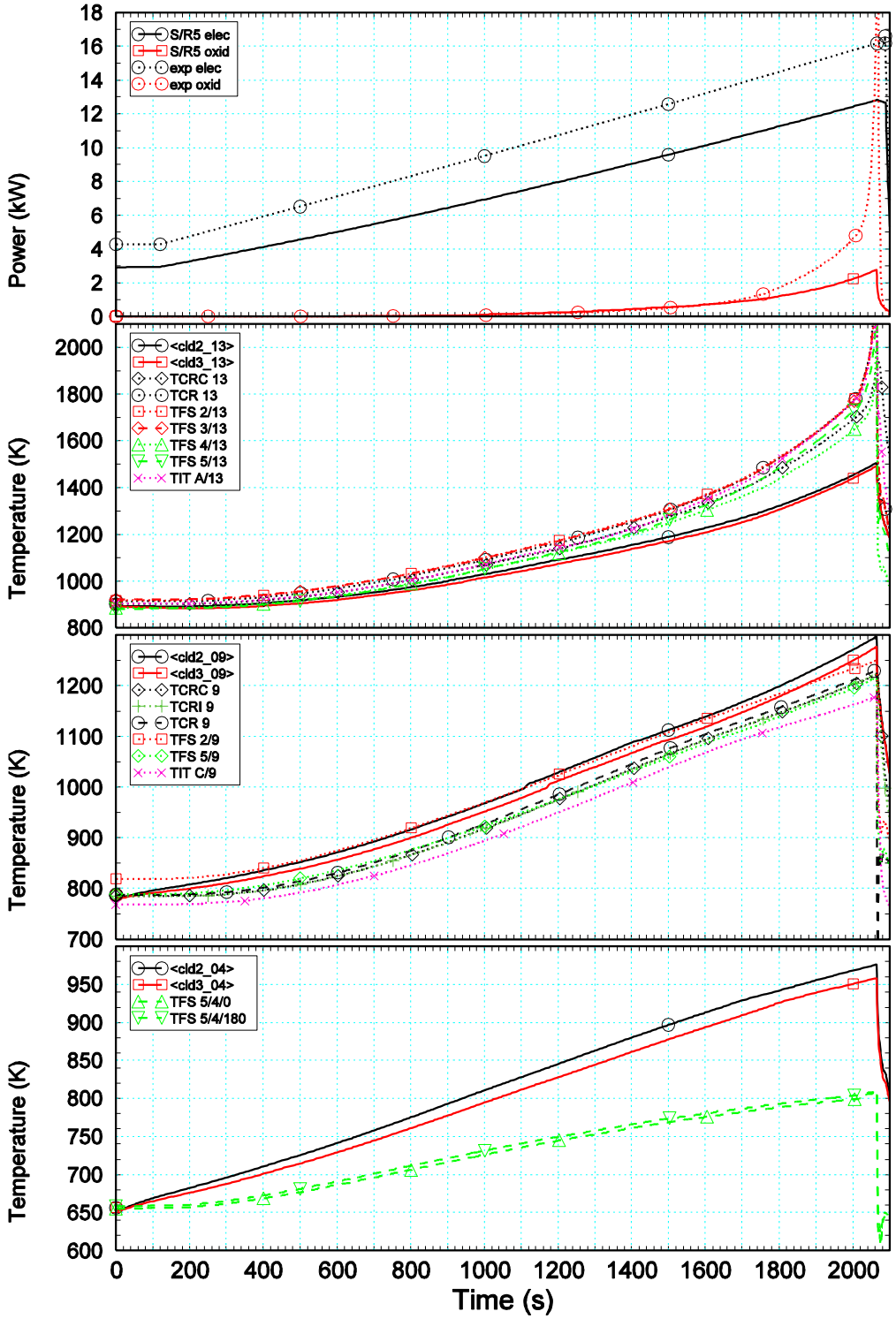

Figure 7 Selected measured and calculated (S/R5) results for QUENCH-04 (I)
The figure shows from top to bottom calculated and measured history of electrical and chemical power and of rod surface temperatures at the top (0.95 m), the center (0.55 m), and the bottom (0.05 m) of the heated length (axial levels 13, 9, and 4, respectively).

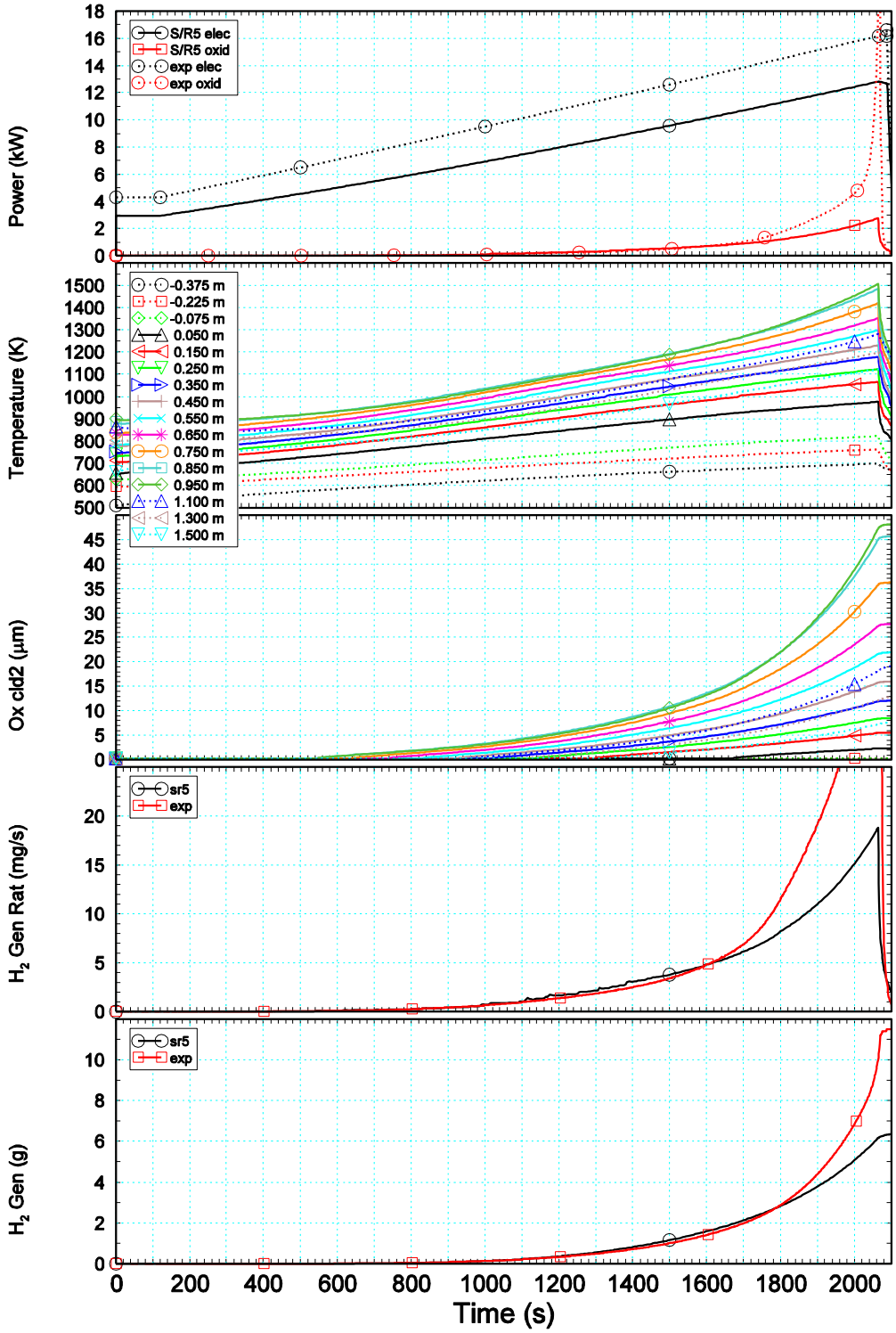

Figure 8 Selected measured and calculated (S/R5) results for QUENCH-04 (II)
The figure shows from top to bottom electrical and chemical power history, calculated surface temperatures of the inner heated rods and oxide scales for the inner heated rods, measured and calculated hydrogen production rate and cumulated hydrogen mass.

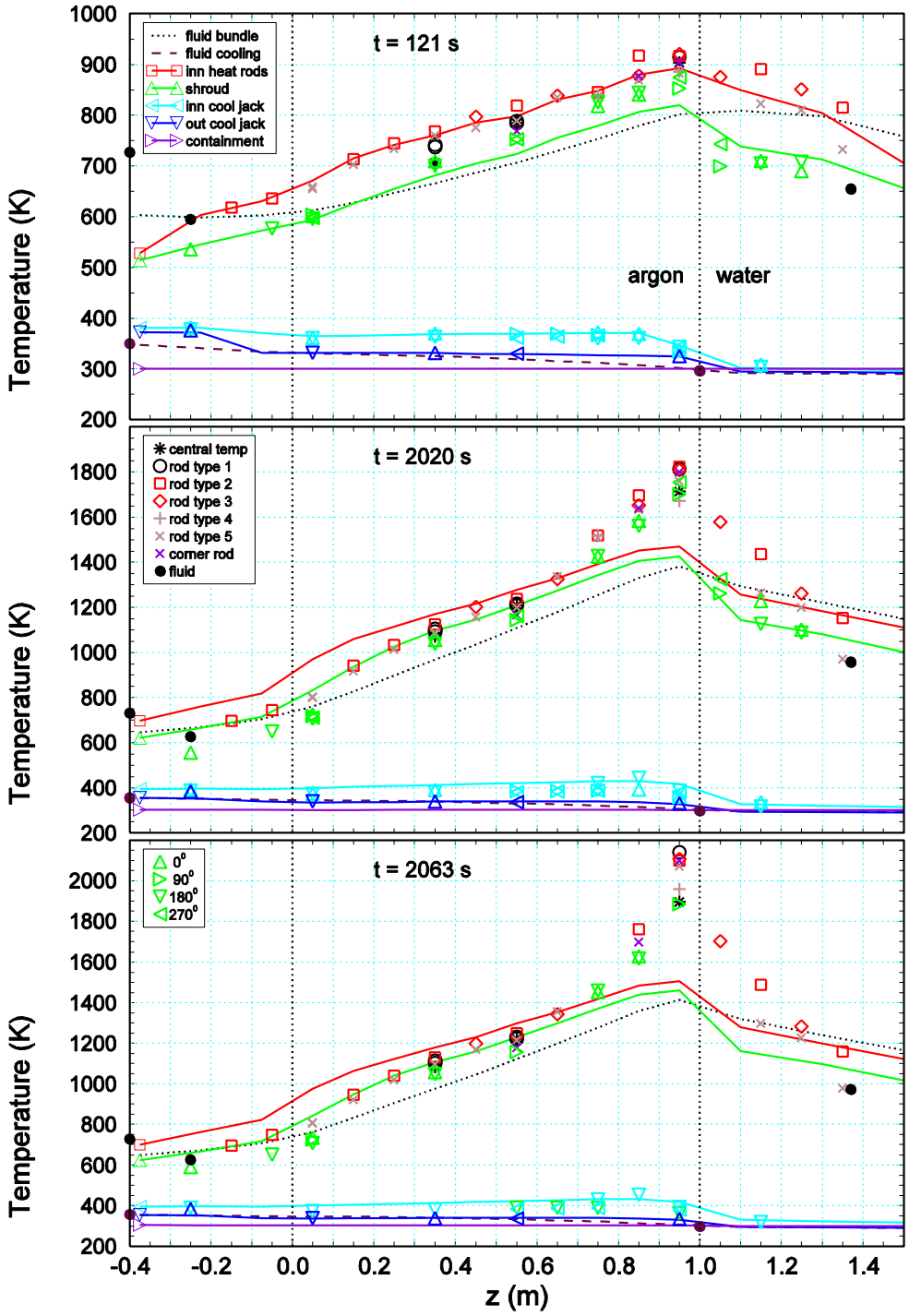

Figure 9 Measured and calculated (S/R5) axial temperature profiles for QUENCH-04
The figure shows from top to bottom temperature profiles at the start of the power transient, the time, when a corner rod was withdrawn, and at the start of the steam cool-down. The meaning of colors for measured (symbols) and calculated (lines) data for the various components is given in the top legend, the azimuthal position of shroud and cooling jacket TCs in the bottom legend.

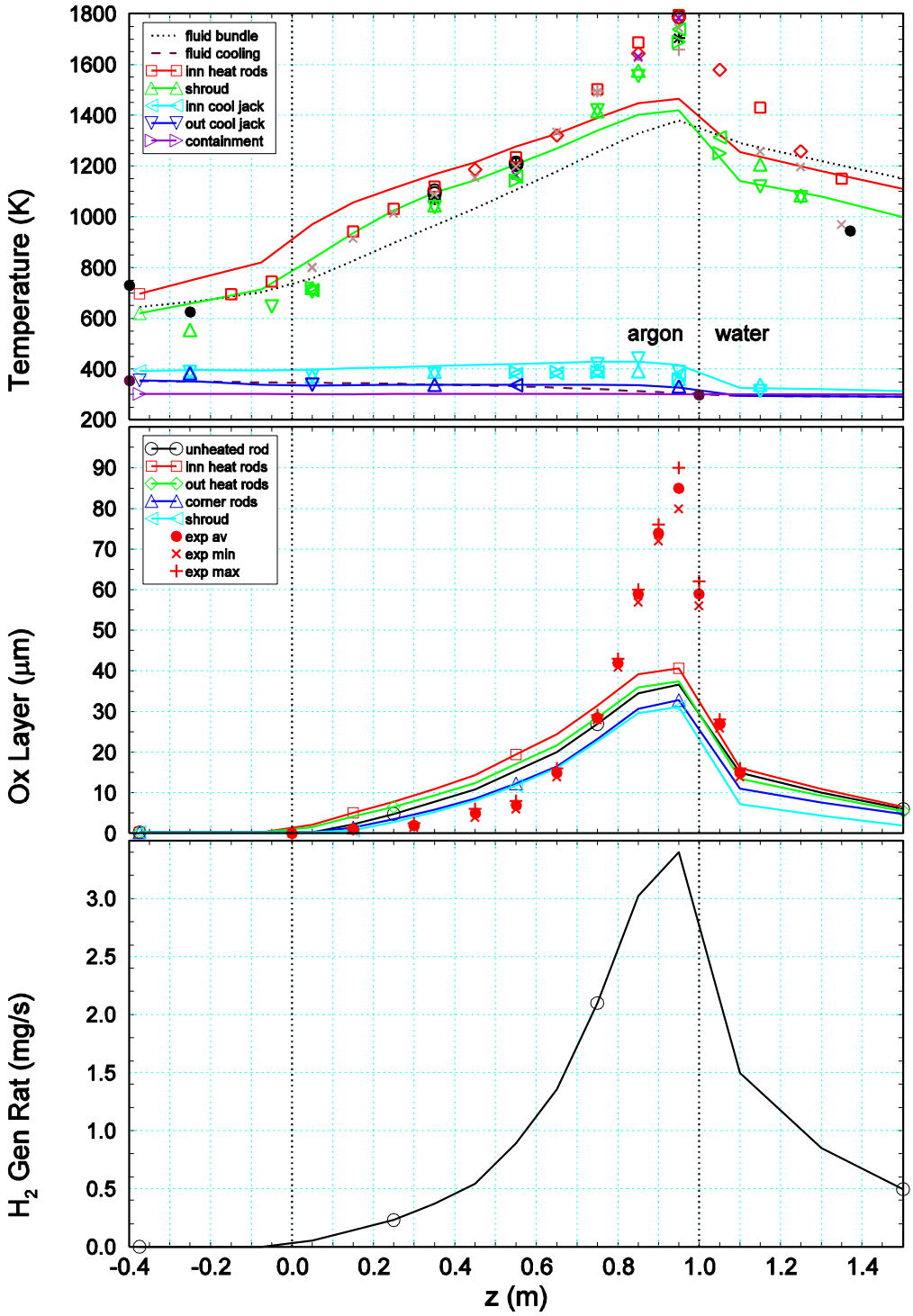

Figure 10 Selected measured and calculated (S/R5) axial profiles for QUENCH-04
The figure shows from top to bottom axial profiles of measured and calculated facility temperatures and oxide scales and calculated hydrogen generation rate at the time, when the corner rod was withdrawn.

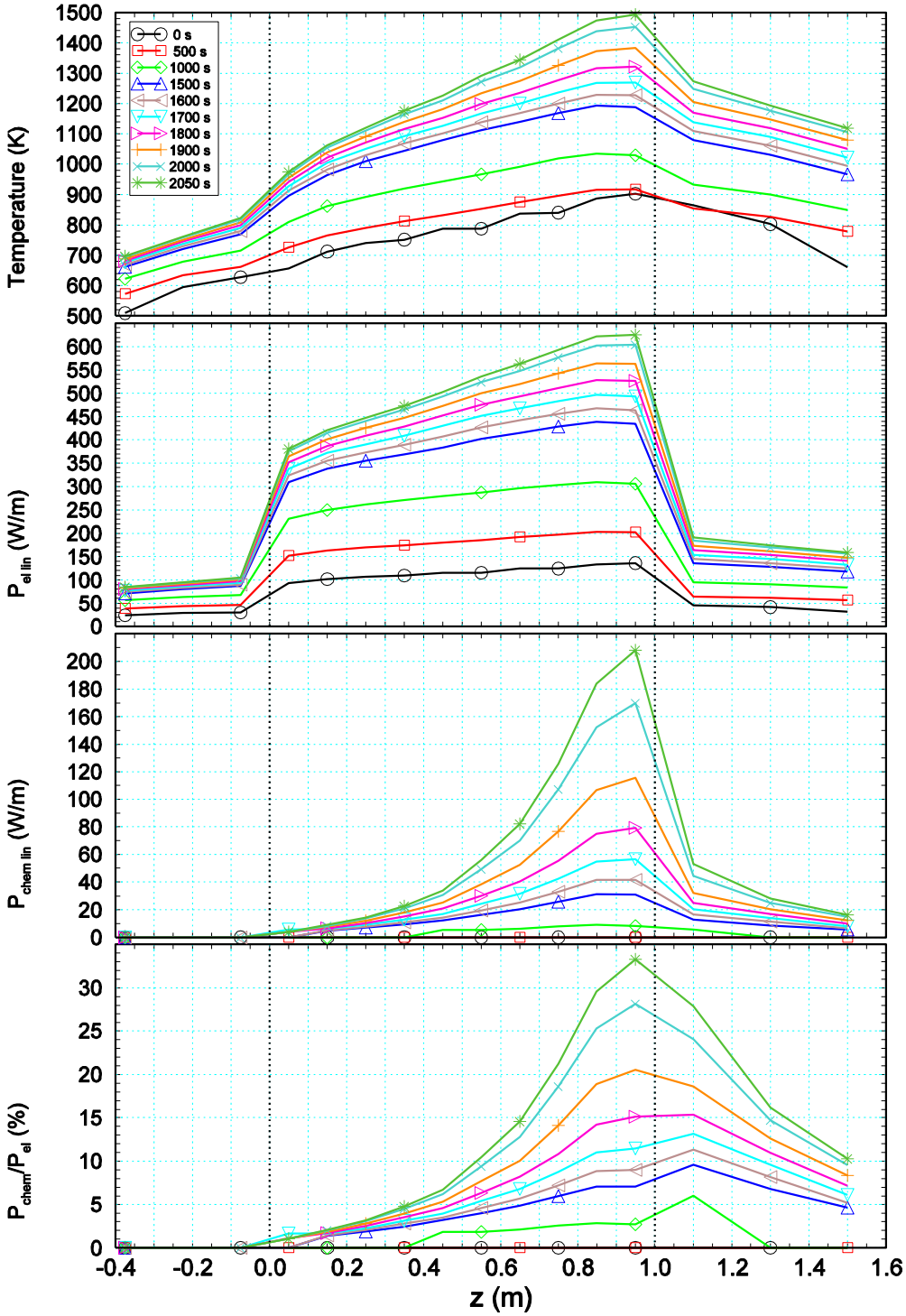

Figure 11 Calculated (S/R5) axial profiles about local power release in QUENCH-04
The figure shows from top to bottom calculated results for the outer surface temperatures for the inner heated rods, linear electrical and chemical rod power release, and their ratio for various times.

4 CALCULATIONS FOR QUENCH-04 WITH RELAP5

It is emphasized that the purpose of the present report is to assess the capabilities of RELAP5 and TRACE and not mainly to present excellent post-test calculations of a given experiment. The test QUENCH-04 is chosen as an experimental basis to be sure that the chosen scenario is reasonable with respect to reactor safety considerations. Though the agreement between the SCDAP/RELAP5 calculations might be improved, the computational results may well serve as a basis for the present investigations. It will be seen that the outcome of the assessment does not depend on the imperfections mentioned above and, furthermore, that a detailed comparison with the SCDAP/RELAP5 calculations should be postponed.

4.1 Modeling of the QUENCH Facility

As far as possible, the SCDAP/RELAP5 modeling has been used for the calculations with RELAP5. However, the SCDAP components for fuel rods, simulators, and shroud have to be replaced by heat structures so that heat conduction can only be considered one-dimensionally instead of two-dimensionally. This is a code limitation for all electrically heated experiments, because the thermal conductivity of the metallic heater elements is by far larger than that of UO_2 so that axial heat conduction cannot be neglected. In addition, the advantage of the detailed electrical heater model [5] is missing in RELAP5. The space between the shroud and the inner cooling jacket in the upper electrode zone, i.e. the region without ZrO_2 insulation, is modeled as a space with stagnant argon.

Since a detailed model for the fuel rod simulators, i.e. the heated rods in the bundle, as in SCDAP/RELAP5 is not available, the local release of electrical power cannot be calculated as a function of local temperature. Therefore, the axial profile for electrical power release has to be prescribed explicitly. For this purpose, SCDAP/RELAP5 results for QUENCH-04 have been used, see Figure 12. Normalized linear rod power shows that the axial profile becomes steeper with time beyond increase of maximum value` with time. This issue has been described in section 3.2 about positive feedback of electrical heaters. In a first step, however, some intermediate axial profile can be used as an approximation, though a better solution as implemented in SCDAP/RELAP5 would be preferable. This approximation is not valid, when a temperature escalation, as it occurs in QUENCH-04 at about 2000 s, has to be taken into account. In the calculations, electrical power input is set such that 72 % of the total electrical power is released in the bundle as for the SCDAP/RELAP5 calculations.

View factors have also been derived from calculations with SCDAP/RELAP5. Oxidation can only be considered for rods, not for the shroud. This code deficiency has a significant drawback on the present application, because the shroud surface corresponds to that of more than seven fuel rod simulators and hence to nearly exactly 25 % of the total oxidizing surface. It makes comparison with experimental data impossible and comparison with SCDAP/RELAP5 results more difficult.

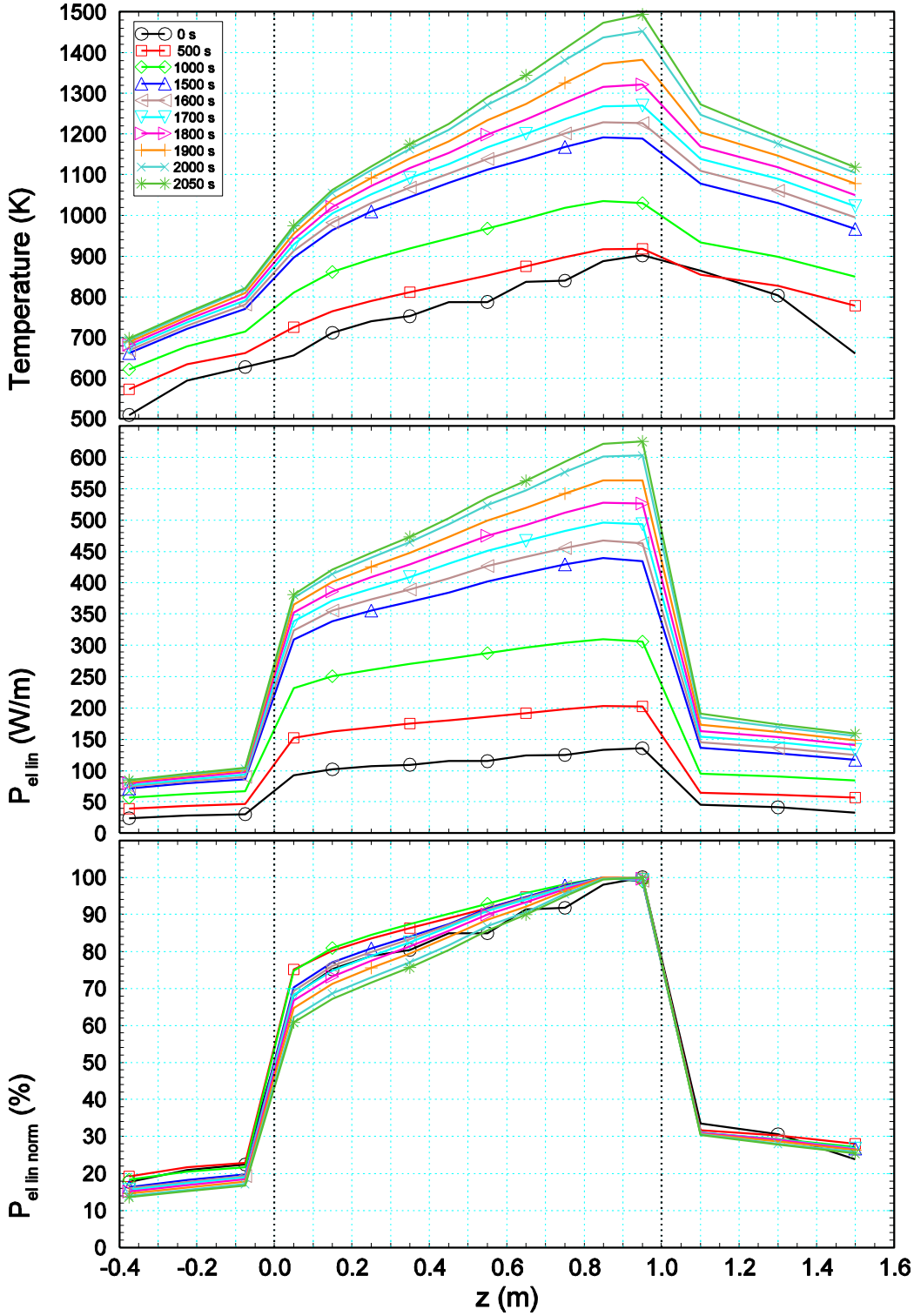

Figure 12 Calculated axial profiles about local electrical power release in QUENCH-04 The figure shows from top to bottom calculated (S/R5) results for the surface temperatures of inner heated rods, real and normalized linear electrical rod power for various times.

4.2 Results

Plot information is scarcer than for SCDAP/RELAP5 calculations. Therefore, most important time dependent results are collected in a single figure, Figure 13, for comparison with experimental data. Temperatures are higher than for SCDAP/RELAP5. This difference is compatible with the lack of axial conduction in RELAP5 heat transfer model. Up to 1560 s, agreement of calculated temperatures with experimental values is quite good, taking in mind the approximations with respect to SCDAP/RELAP5. The calculated and measured radial profiles are similar. At that time, a sharp temperature step of nearly 50 K is calculated for the inner heated rods at the upper end of the heated zone. A similar temperature step is calculated for the outer heated rods at 1575 s and for the unheated central rod at 1590 s. Figure 14 shows that other axial levels are not involved. This can be seen even more clearly in Figure 15, where the derivatives with respect to time are given. After the temperature step, temperature increases smoothly, but becomes faster and faster, until code failure at 1755 s. Experimental results is grossly overestimated after the temperature step.

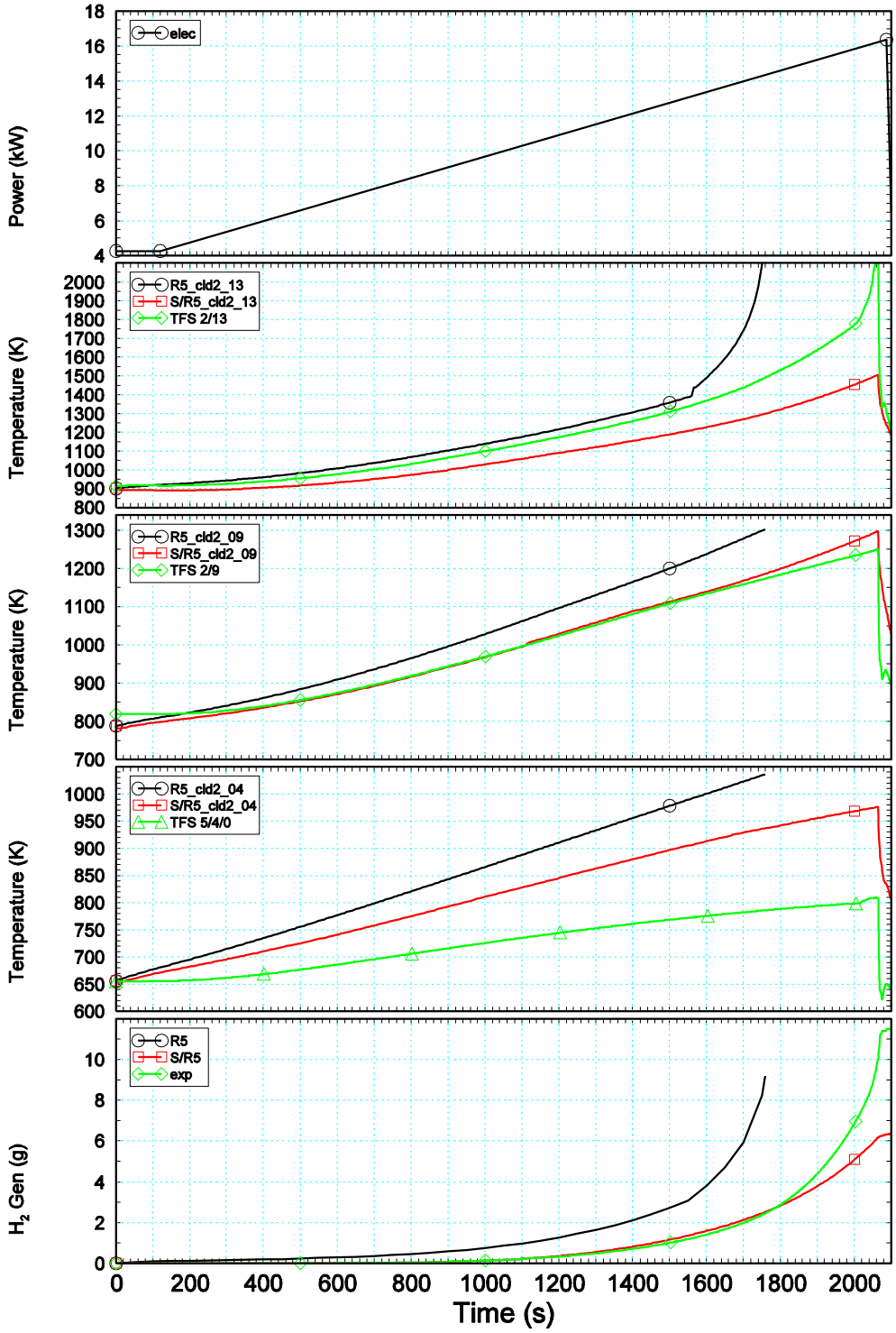

Figure 13 Selected measured and calculated (R5) results for QUENCH-04
The figure shows from top to bottom history of total facility power and surface temperatures of the various bundle components at the top, the center, and the bottom of the heated length (axial levels 13, 9, and 4, respectively) and cumulated hydrogen mass.

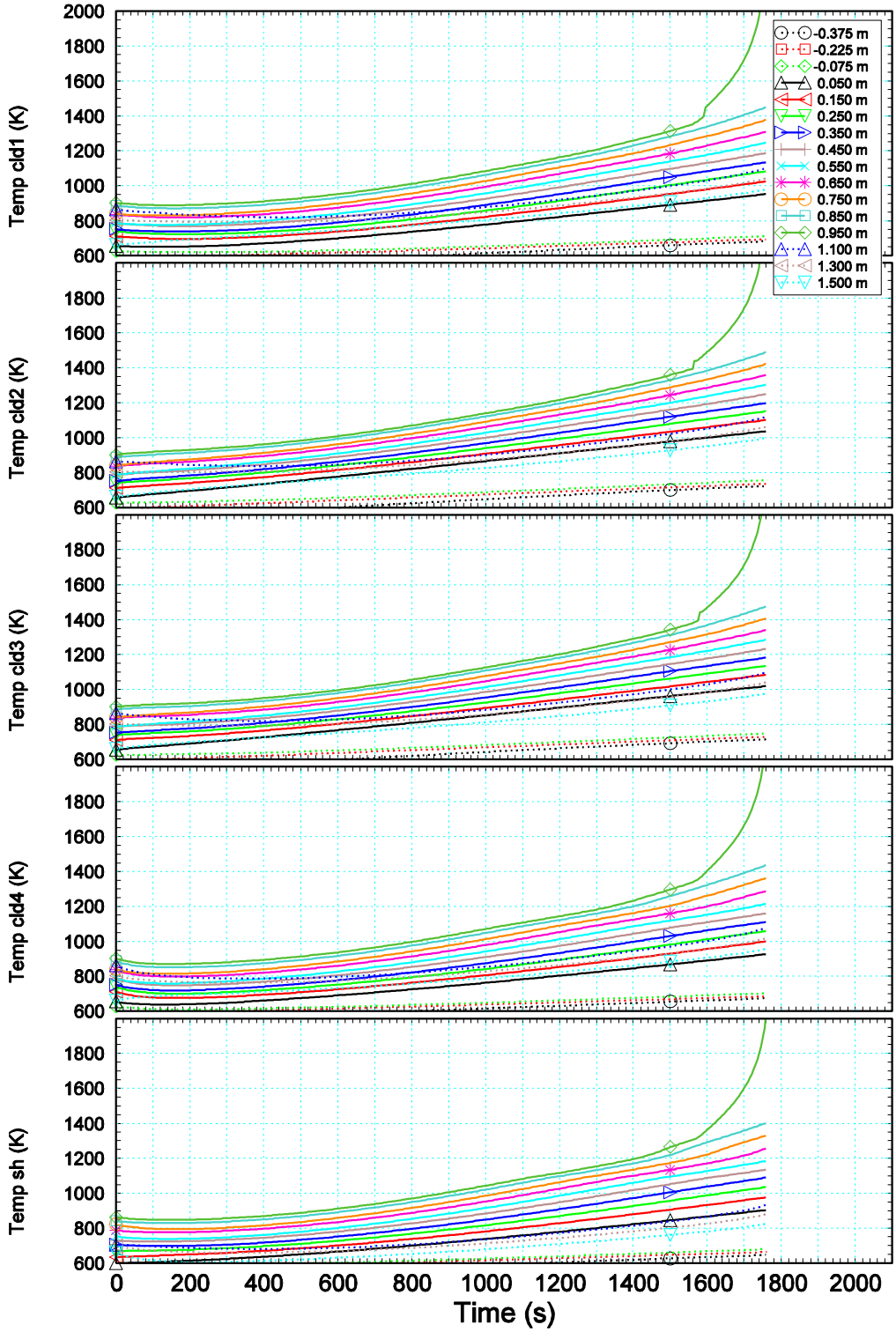

Figure 14 Calculated (R5) rod and shroud temperatures for QUENCH-04
The figure shows from top to bottom surface temperatures at all axial levels of the various bundle components.

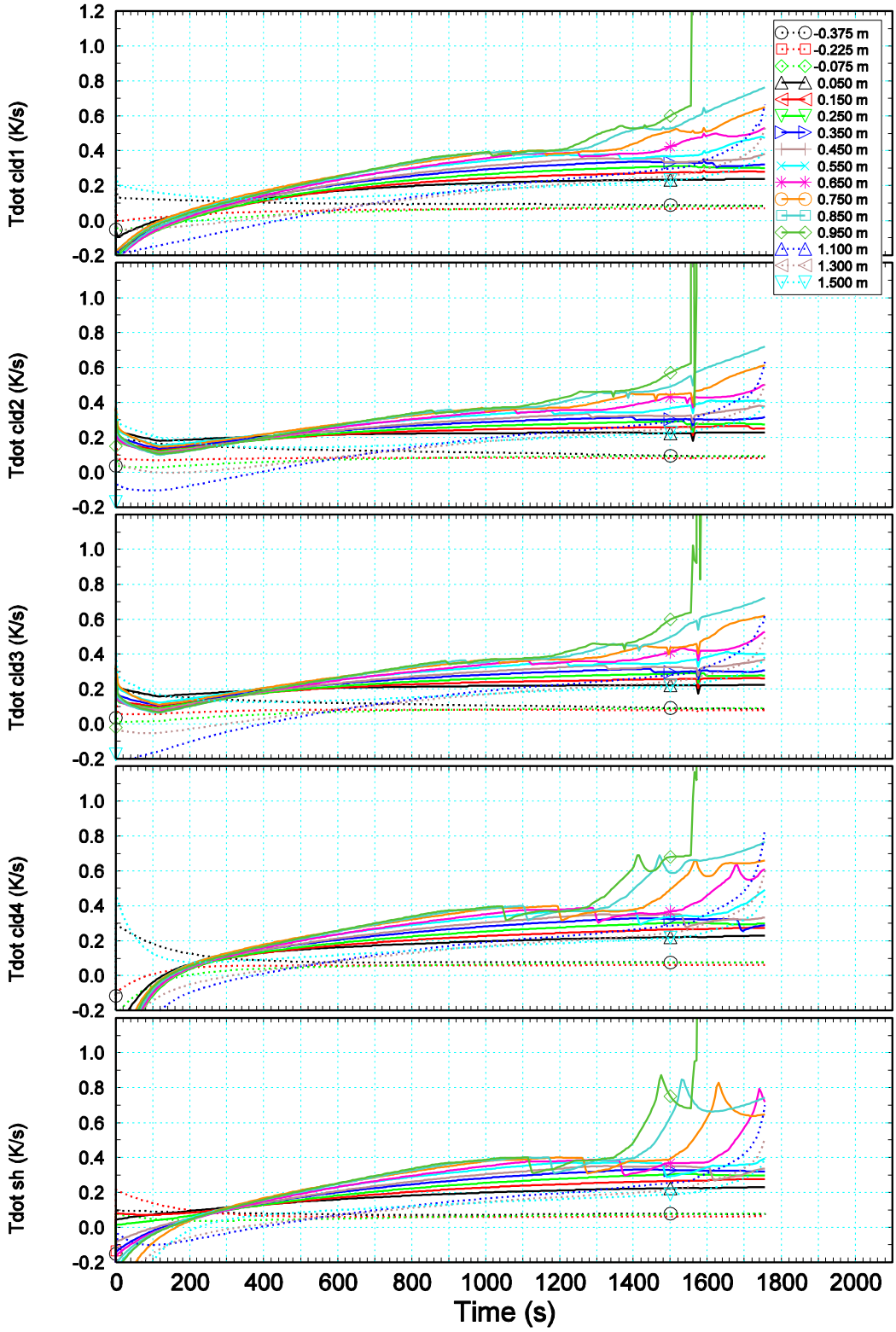

Figure 15 Calculated (R5) temperature derivatives for QUENCH-04
The figure shows the derivatives of the rod and shroud temperatures, shown in Figure 14.

5 CALCULATIONS FOR ALTERNATE BUNDLE WITH RELAP5

5.1 Modeling of the Alternate Bundle

Figure 16
Nodalization of alternate bundle with RELAP5

Since the sharp temperature step at 1560 s and the subsequent overestimated temperature increase are not acceptable, this error was examined in more detail. In a number of steps, those parts of the original input deck were isolated that are essential for the error; all other parts are deleted. In the final version, only a bundle, similar to the original geometry, with time dependent volumes and junctions at its ends are taken into account (Figure 16); the lower plenum, argon and water inlet, the components outside the shroud and the off-gas pipe are not modeled (Figure 6).

In detail, the bundle is modified to some aspects with respect to the experimental conditions of QUENCH-04. Sixteen axial meshes are used as before, but all with the same length of 0.1 m. The corner rods are modeled to be identical to the unheated central rod; the shroud diameter is increased for geometric consistency. The spacer grids are not considered. The bundle is modeled to be in an adiabatic Zircaloy shroud. Radiation heat exchange is not taken into account. The steam mass flow rate is constant at 3 g/s with a constant inlet temperature of 620 K. Initial temperatures of the heat structures are modified because of the above changes. Their axial profiles are the same for all rods and the shroud. Because of the modifications, calculated temperatures in the inner and outer heated rods and of the central and the corner rods, respectively, are the same.

Two calculations are done for the alternate bundle up to the start of the steam cool-down phase, one without and one with rod oxidation, cases A and B, respectively. As mentioned in section 4.1, the oxidation model can only be activated for rods but not for the shroud. In calculations for the alternate bundle with SCDAP/RELAP5, done for comparison, the same input deck is used as for RELAP5 except for some minor formal changes. This means, that in these SCDAP/RELAP5 calculations, shroud oxidation is also suppressed. Data for the various calculations, including those with TRACE, are listed in Table 1. The different computers, used for the various calculations, reflect that the work has been performed over a longer time period and that the available resources were used for simplicity instead of implementing all codes on the same platform. The cpu times show that the chosen input model give fast results. The differences in computing times on the various computers also demonstrates that the computer architectures has a marked influence on the code performance.

The electrical power input is modified with respect to the original QUENCH-04 case so that for both cases (with and without oxidation), the maximum bundle temperatures and hence hydrogen production are similar to those of the original QUENCH bundle in the temperature range of interest for RELAP5. In later times, very high temperatures may be reached.

Since in case A the maximum temperature is a result of electrical power release alone and in case B of combined electrical and chemical power release, additional electrical power is required in case A to reach the same maximum temperature as in case B. In later times into the transient, electrical power in case A is therefore markedly higher than in case B.

Table 1 List of cases, calculated with the various codes

Code	case	ox	P_{max} (kW)	t_{end} (s)	cpu time (s)	computer
SCDAP/ RELAP5	A	-	40	2063.0	28.92	IBM pSeries Power 4, 1,5 GHz
	B	+	15	1842.4	26.58	
RELAP5	A	-	40	2063.0	139.58	Intel Xeon, 2.4 GHz
	B	+	15	1943.3	138.21	
TRACE	A	-	40	2063.0	94.59	Intel 2, 2.93 GHz
	B	+	15	2063.0	97.69	
	C	+	40	2063.0	96.09	

case A without oxidation model
case B with oxidation model
case C with oxidation model, power history as in case A
ox oxidation model on/off (redundant information for better readability)
P_{max} maximum total electrical power
t_{end} maximum problem time

The time step is 50 ms for all calculations. SCDAP/RELAP5 case B ends abnormally, when the upper temperature limit of 2500 K in material property data is exceeded, demonstrating that no error during program execution occurs before. RELAP5 case B ended abnormally due to a fatal error during program execution.

This modeling of electrical power history in the two cases can only be approximated, because heat release due to oxidation is largely restricted to the hot region at the upper end of the heated zone, whereas electrical power release varies by far less in the heated part of the bundle, see central part of Figure 11. Therefore, changes of the electrical power also affect the lower part of the bundle. Some more efforts for a better presentation of the real QUENCH case might have been done, but taking in mind the above limitations of the model, further efforts did not seem to be justified for the present investigation.

5.2 Results

When the oxidation model is deactivated (case A), temperatures differ somewhat with respect to the related SCDAP/RELAP5 calculation. These differences increase with time, but they are always below 15 K. This is an indication that there may be small differences in the two codes, but the input deck is interpreted essentially in the same way in the two codes.

Whereas no problem was detected in the calculation without oxidation, the code ends abnormally at 1943 s due to very high temperatures. As for the original QUENCH case, there is a steep and sudden temperature increase of 50 K and more at one axial level, but neither at the upper end of the heated zone nor at the same level for heated and unheated rods (Figure 17). The derivatives of temperature with respect to time at other axial levels are interpreted as a consequence of the temperature step at a single level (Figure 18). For the heated rods, it is at axial level 8 at 1893 s, for the unheated rods it is even at axial level 12 at 1921 s.

The axial temperature profiles (Figure 19) show the increasing influence of oxidation. As expected, it occurs mainly in the hot zone. Due to the higher temperature, it is largest in the heated rods. In the lower part of the heated zone, calculated temperatures are higher in case A (without oxidation) than in case B, the effect being larger later in the transient. This effect is due to the different electrical power input in cases A and B. In case A, electrical power is higher to compensate for the lacking release of chemical power. The latter is essentially restricted to the hot zone, but the increase of electrical power is applied to the whole bundle length, as explained in section 3.2 and at the end of section 5.1, leading necessarily to higher temperatures at the bottom of the heated length. The effect would even be higher, when the maximum temperatures in cases A and B would be closer together by some more efforts to prescribe the electrical power history.

A comparison of axial temperature profiles, calculated with RELAP5 and SCDAP/RELAP5 (Figure 20), shows that the results are nearly the same as long as oxidation is negligible. SCDAP/RELAP5 results are higher later into the transient. The difference reflects the different oxidation models in RELAP5 and SCDAP/RELAP5. The high maximum temperature at 1800 s, calculated with SCDAP/RELAP5, is probably mainly due to a change of the oxidation model at 1853 K from the Cathcart correlation to that of Urbanic and Heidrick [3]. It gives higher oxidation rates than the various low-temperature correlations [11]. Since RELAP5 and TRACE are not developed for this temperature range, there is no change of the oxidation model in these two codes.

The results of the calculations suggest that the oxidation model in RELAP5 has a severe error. It is not correlated directly with temperature.

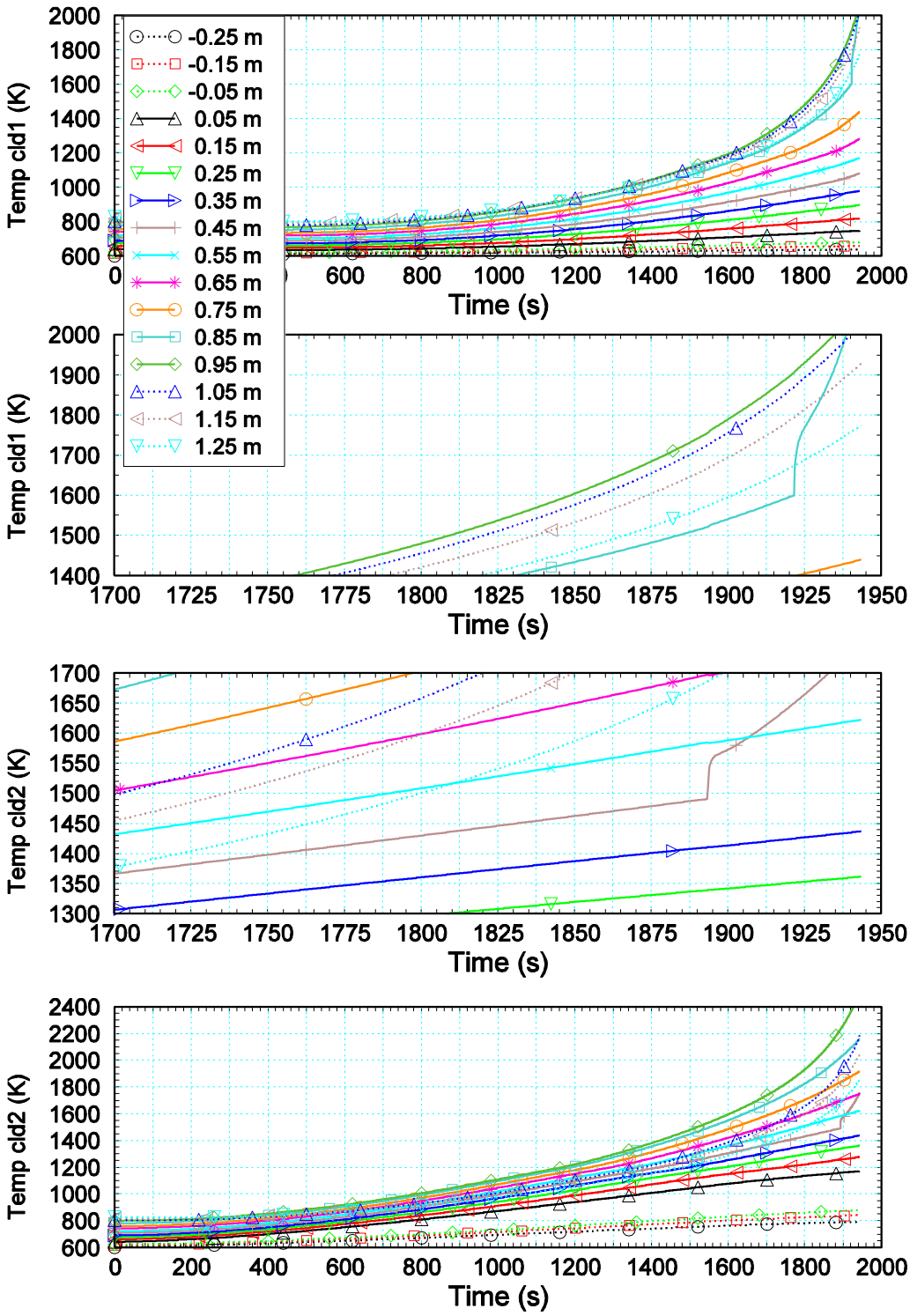

Figure 17 Calculated (R5) temperatures for case B
At top and bottom, the figure shows outer surface temperatures at all axial levels in the bundle for the unheated central rod and the inner heated rods, respectively. Details for both rod typs are given in the central part of the figure.

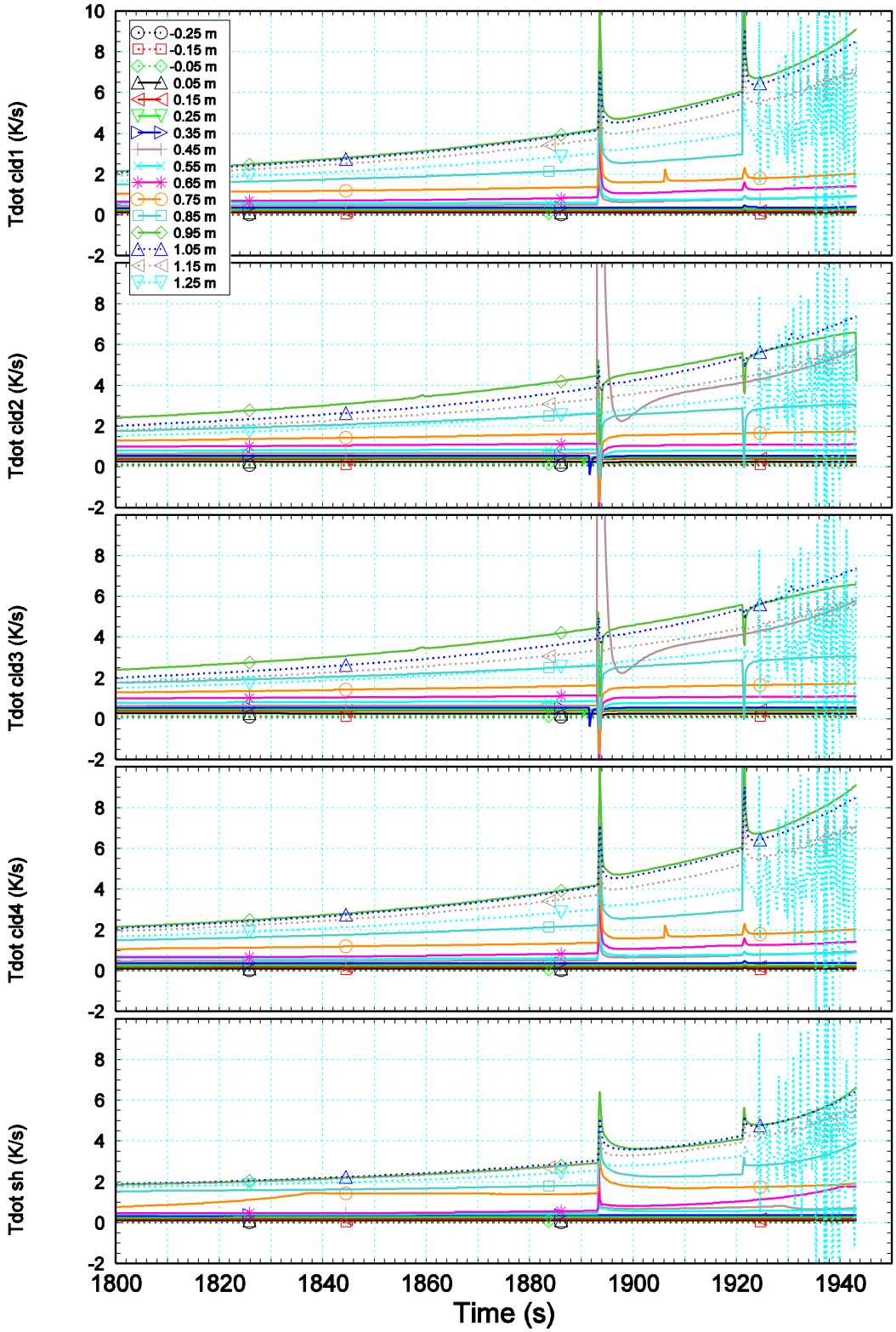

Figure 18 Calculated (R5) temperature derivatives for case B
The figure shows the derivatives of the rod and shroud temperatures, shown in Figure 17.

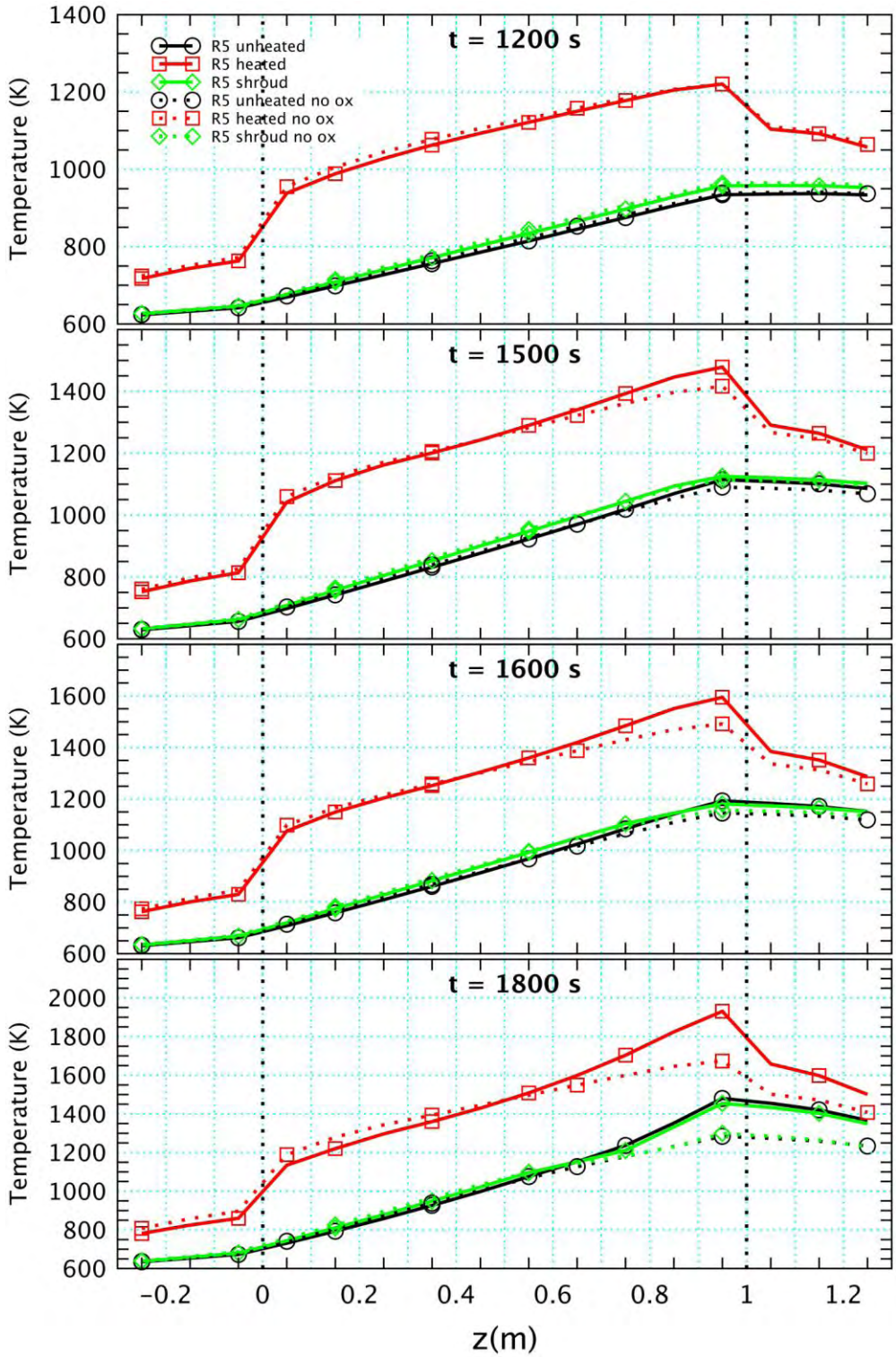

Figure 19 Axial profiles for cases A and B with R5

The figure shows axial temperature profiles of the unheated and heated rods, and the shroud at various times.

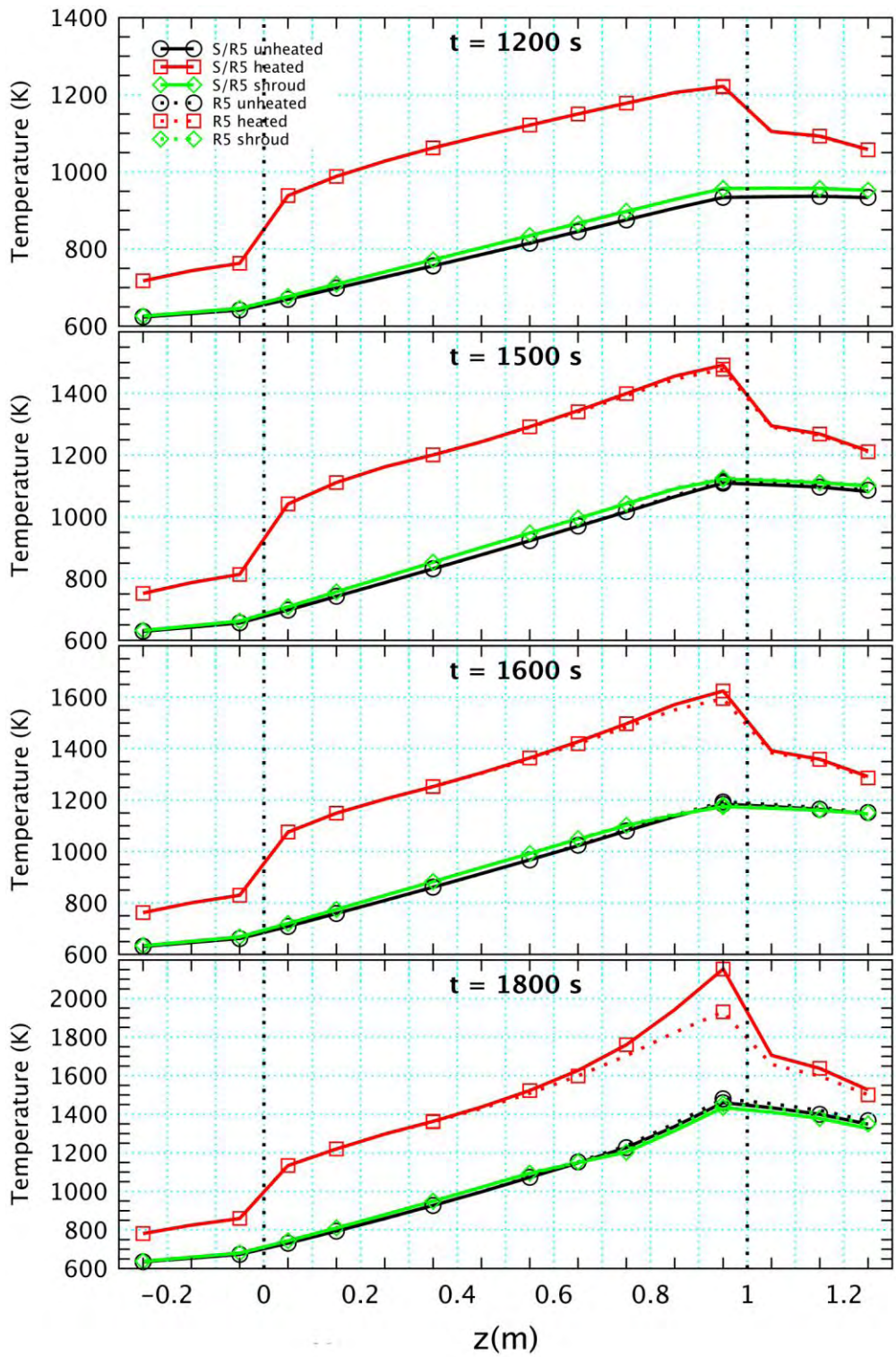

Figure 20 Axial profiles for case B with S/R5 and R5

The figure shows axial temperature profiles of the unheated and heated rods, and the shroud at various times.

6 CALCULATIONS FOR ALTERNATE BUNDLE WITH TRACE

The two cases for RELAP5 calculations have been transformed into TRACE input decks with SNAP, version 1.2.0 [7] so that the same geometrical and physical configuration is considered. Some changes of the new input deck had to be done manually because of error messages during program execution. They concern control variables, used for printout in RELAP5, variable ielv for definition of axial discretization, and activation of the oxidation model. In addition, the axial electrical power profile is interpreted wrongly in two ways. Firstly, the total electrical power, as given in a table, is used to 100 % for the rods and not to 72 % as in RELAP5, and secondly, the total power, given in the table for the whole bundle, is applied for the inner heated rods and the same total power is applied for the outer heated rods. Some other changes were added to tighten the input deck, e.g. to replace the two components “BREAK” and “PUMP” by a single “FILL”. During the work, it was found that plot information is inferior to RELAP5 possibilities.

Case A (without oxidation) gives similar temperature results for the upper end of the heated zone as with RELAP5 (Figure 21). Temperatures of the heated rods at the upper end of the heated zone are calculated to be somewhat lower with TRACE than with RELAP5, but the difference is rather small at the end of the transient. The derivative of temperature with respect to time shows that temperature is smooth as it should be.

Axial profiles (Figure 22) show that in TRACE and RELAP5 different temperature profiles are calculated. The difference is larger at lower axial positions, its maximum being at the lower end of the heated zone. In contrast, temperatures of unheated rods and of the shroud are higher in TRACE than in RELAP5, the maximum difference being around the center of the heated length. Similar large differences occur at the lower end of the lower electrode zone. The reason for these differences could not be identified; it might at least partly have to do with a different modeling of the radial distribution of the heat source in the two codes. In RELAP5, the radial distribution for power release is restricted to the tungsten heater for the calculations in this report, whereas in TRACE, power released is smeared in the radial direction in the rods.

For case B (with oxidation), the run ends normally, but larger differences occur with respect to RELAP5 and SCDAP/RELAP5 calculations. Temperature rise is far less in TRACE: maximum rod temperature at the end of the calculation is only 1739 K (Figure 23). In case A, temperatures are higher than in case B at all axial levels, for heated and unheated rods and for the shroud (Figure 24) and even as early as at 1200 s. This is in contrast to RELAP5 results (see Figure 19). This finding suggests that release of chemical power due to oxidation is not treated correctly in TRACE. The higher temperatures in case A would then be attributed to the different electrical power release in both cases; it is higher in case A already at 1200 s (Figure 23).

To get some more insight, case B was modified insofar that the same power history was applied as in case A, the case without oxidation, and this new case is called case C. Temperature at the upper end of the heated zone is now generally higher in case C (Figure 25) and calculated hydrogen production is higher. As it is expected, differences between cases A and C occur mainly near the upper end of the heated zone (see the axial temperature profiles Figure 26), because it is only there that oxidation plays a role. In early times of the transient, the temperature at the upper end of the heated zone is the same as without oxidation, because oxidation is not yet calculated or because oxidation is still negligible. Afterwards, the temperature increase is far less: temperature at the upper end of the heated zone and hence maximum rod temperature is only about 170 K higher at the end of the calculation than without oxidation and hence far less than

expected from RELAP5 and SCDAP/RELAP5 experience. This is clearly demonstrated in Figure 27 and Figure 28, where temperatures of heated rods in TRACE are always significantly below RELAP5 results.

A closer look to the results shows that oxidation starts at different temperatures and hence at different times in SCDAP/RELAP5 and TRACE: 3 g hydrogen are calculated to be released in RELAP5 and SCDAP/RELAP5, before oxidation is assumed to start in TRACE, but this difference cannot explain the large discrepancies at later times. It further shows that in the TRACE calculations with and without oxidation, temperatures are the same until the peak in the derivative of temperature with respect to time occurs at 1335 s (Figure 25). At other axial levels, rod and shroud temperatures are the same for a longer time. The peak indicates a steep temperature increase, but it is by far smaller than in the RELAP5 calculations.

A comparison of Figure 21, Figure 23, and Figure 25 shows that the mass error does not differ much, irrespective of whether the oxidation model is activated or not. It also shows that the TRACE mass error changes is less than that in RELAP5 and that RELAP5 mass error is about the same as in SCDAP/RELAP5 as far as no code problem occurs.

To tackle further the problems of the oxidation model in TRACE, the difference between centerline rod and clad outer surface temperature for heated rods was calculated at the top, the center, and the bottom of the heated zone. For comparison, this was done for RELAP5 and SCDAP/RELAP5 for the case with oxidation and for all three cases, calculated with TRACE. RELAP5 and SCDAP/RELAP5 results are similar except at the top of the heated zone at the end of the transient. In any case, the centerline is colder than the clad surface. In contrast, the centerline temperature is calculated with TRACE to be higher, and the absolute values of the temperature differences are approximately the same only in the center of the heated zone. It is possible that this different behavior has to do with a different modeling of the radial distribution of the heat source as it was suggested [14], but the overall result suggests that the problem is somewhat more difficult.

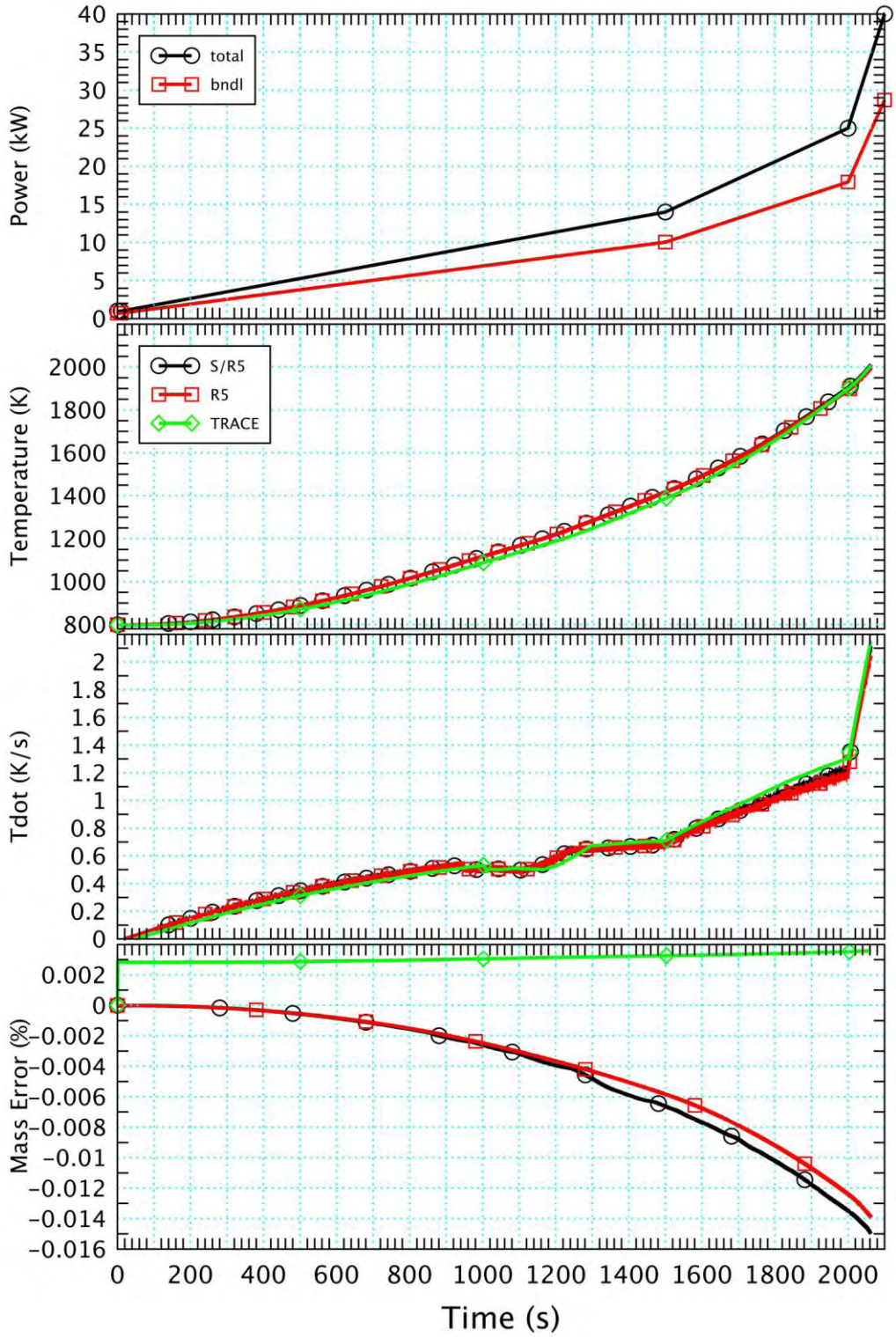

Figure 21 Comparison of case A with TRACE, R5, and S/R5
The figure shows from top to bottom electrical power history, temperature of the inner heated rods at the upper end of the heated zone, related time derivatives, and mass errors.

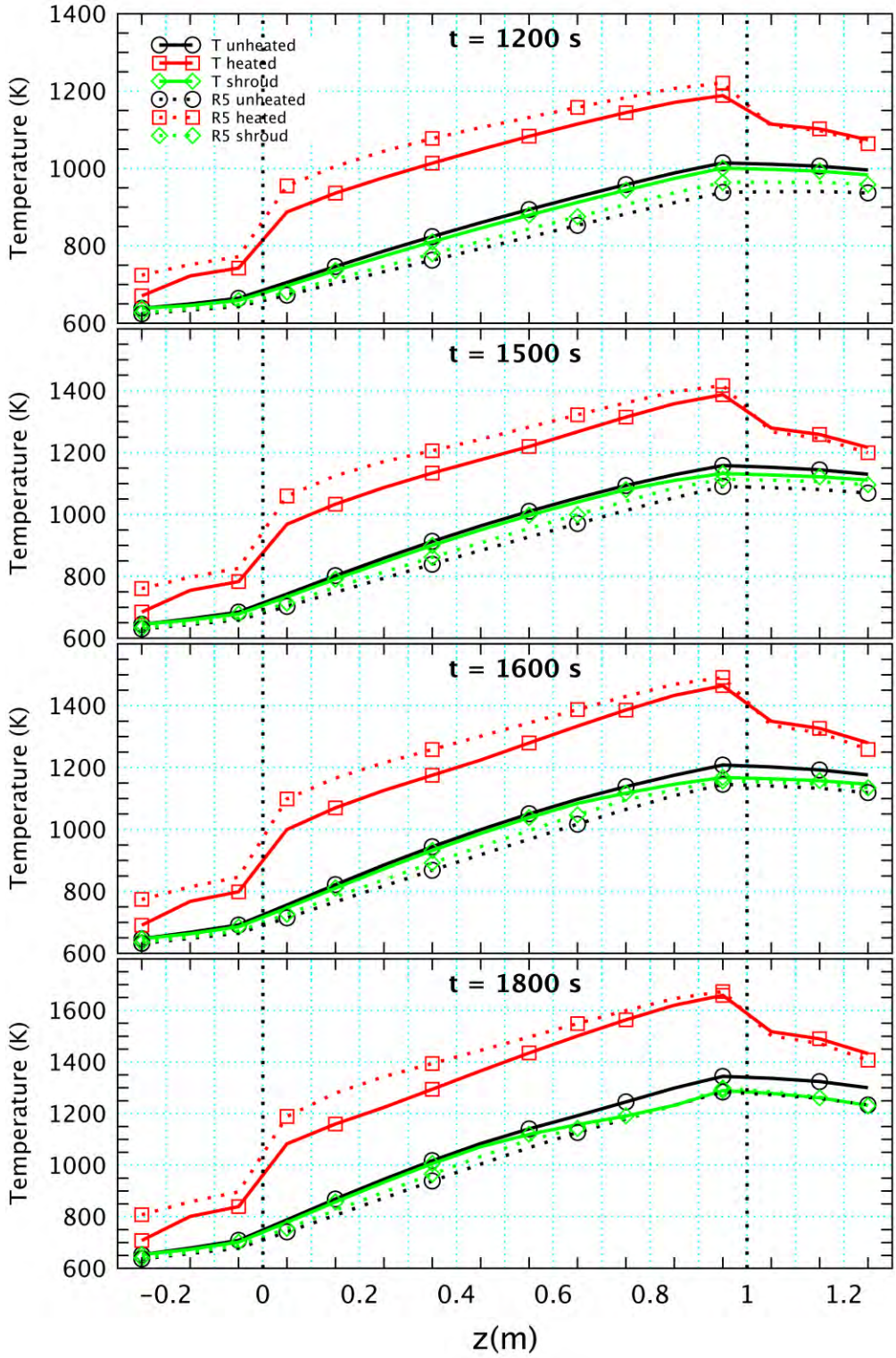

Figure 22 Axial profiles for case A with TRACE and R5
The figure shows axial temperature profiles of the central rod, the inner heated rods, and the shroud at various times.

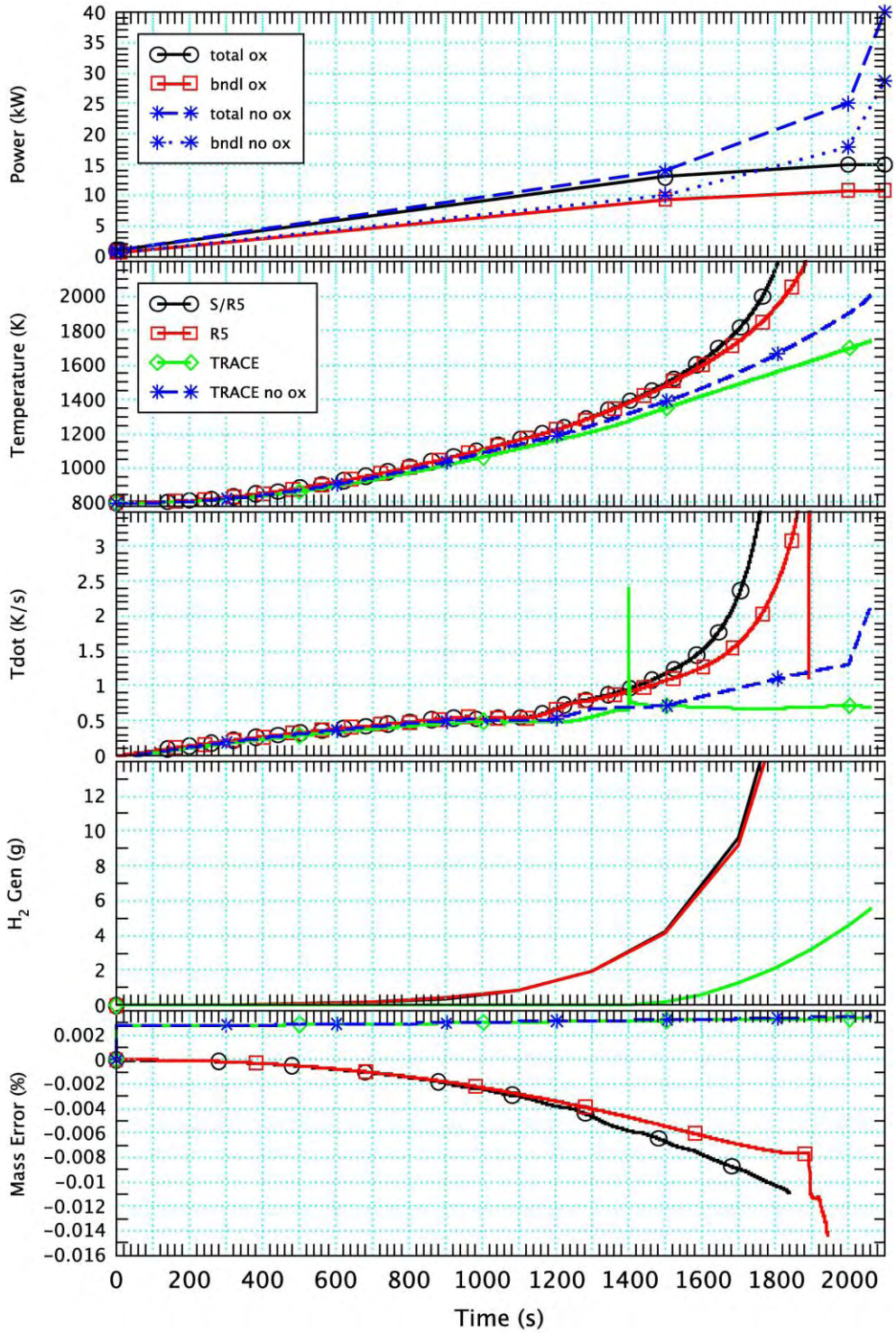

Figure 23 Comparison of case B with TRACE, R5, and S/R5

The figure shows from top to bottom electrical power history for the cases with and without oxidation, surface temperatures of the inner heated rods at the upper end of the heated zone, related time derivatives, cumulated hydrogen mass and mass errors.

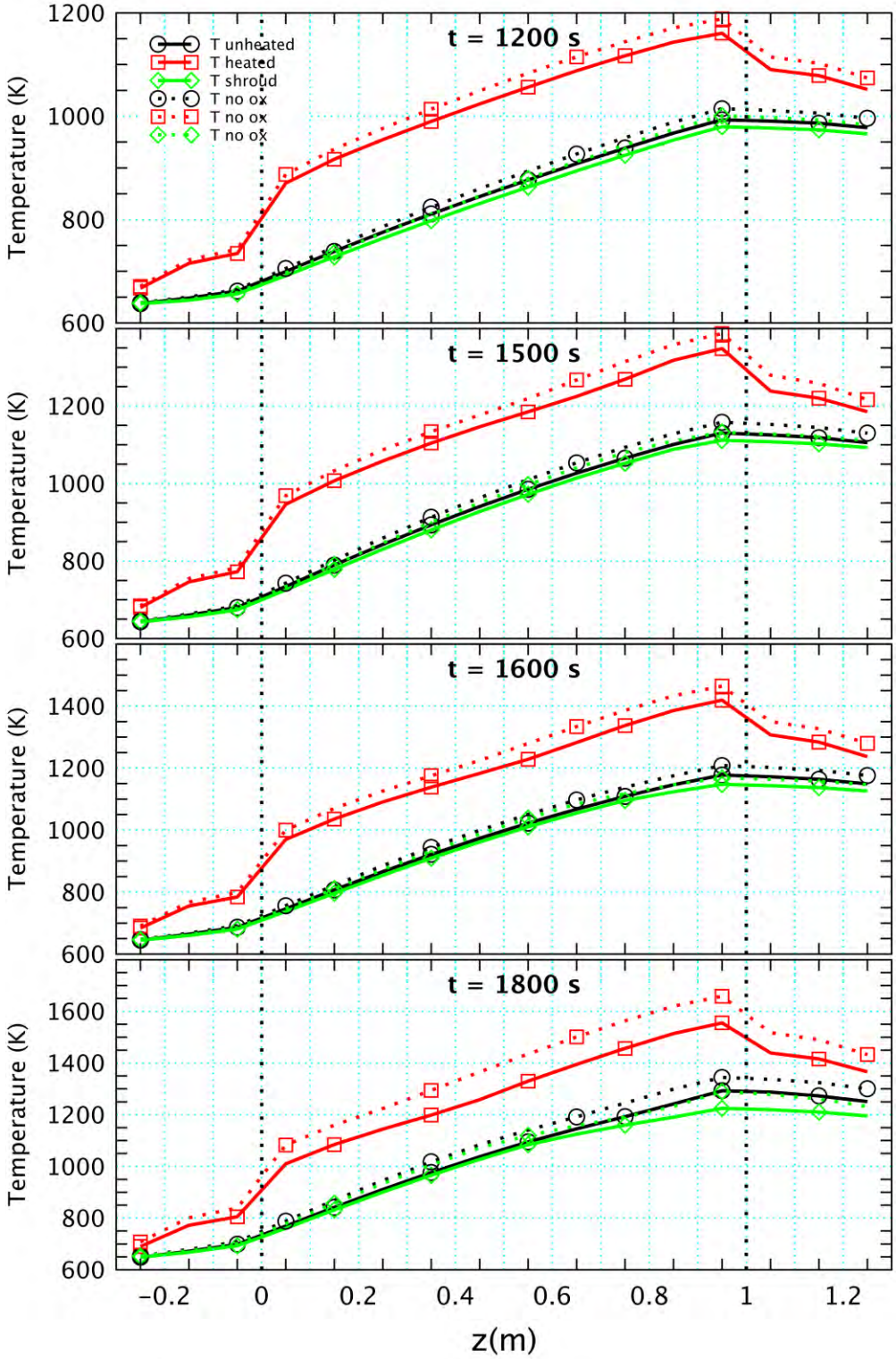

Figure 24 Axial profiles for cases A and B with TRACE
The figure shows axial temperature profiles of the central rod, the inner heated rods, and the shroud at various times.

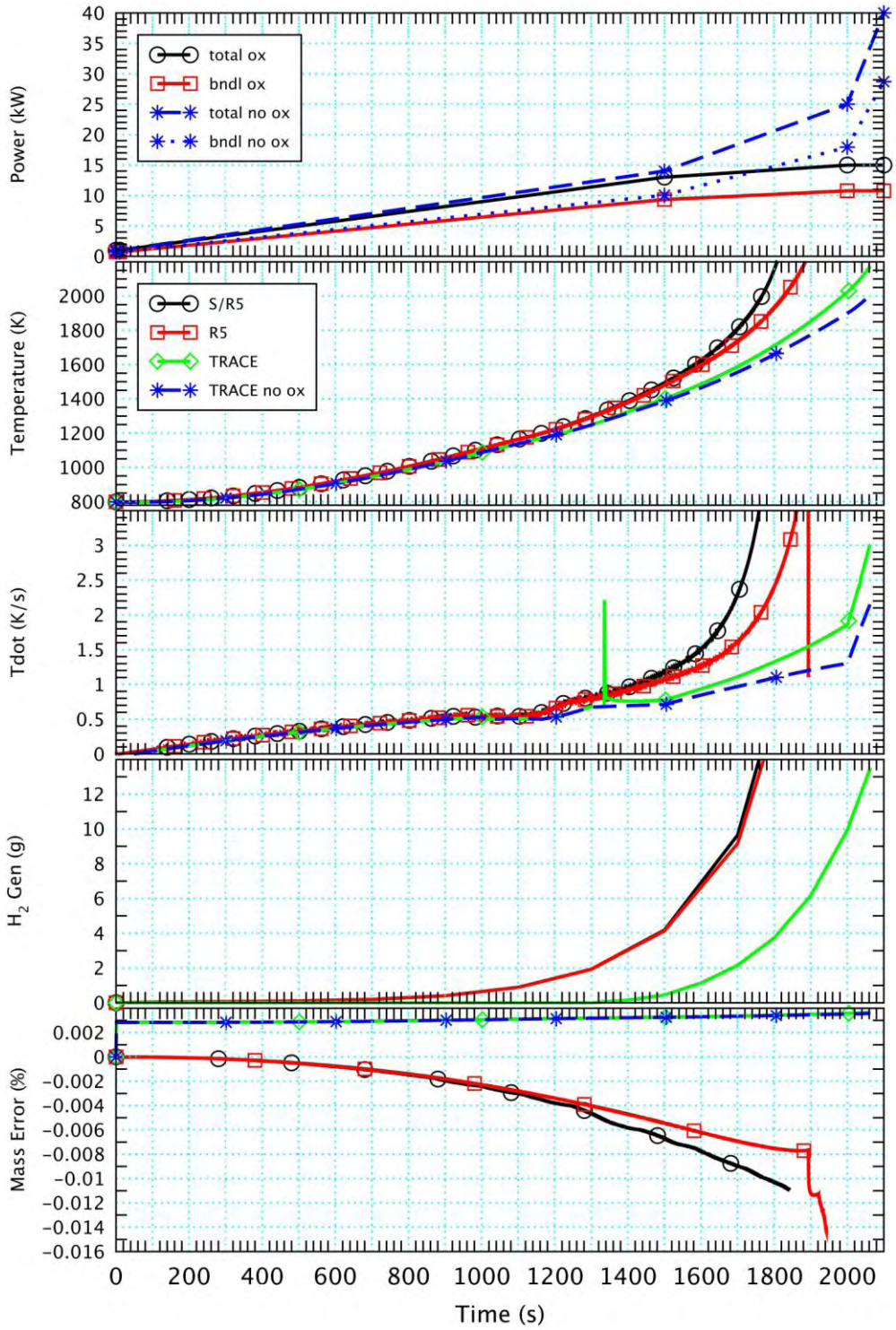

Figure 25 Comparison of case C with TRACE, R5, and S/R5
The figure shows from top to bottom electrical power history for the cases with and without oxidation, surface temperatures of the inner heated rods at the upper end of the heated zone, related time derivatives, cumulated hydrogen mass and mass errors.

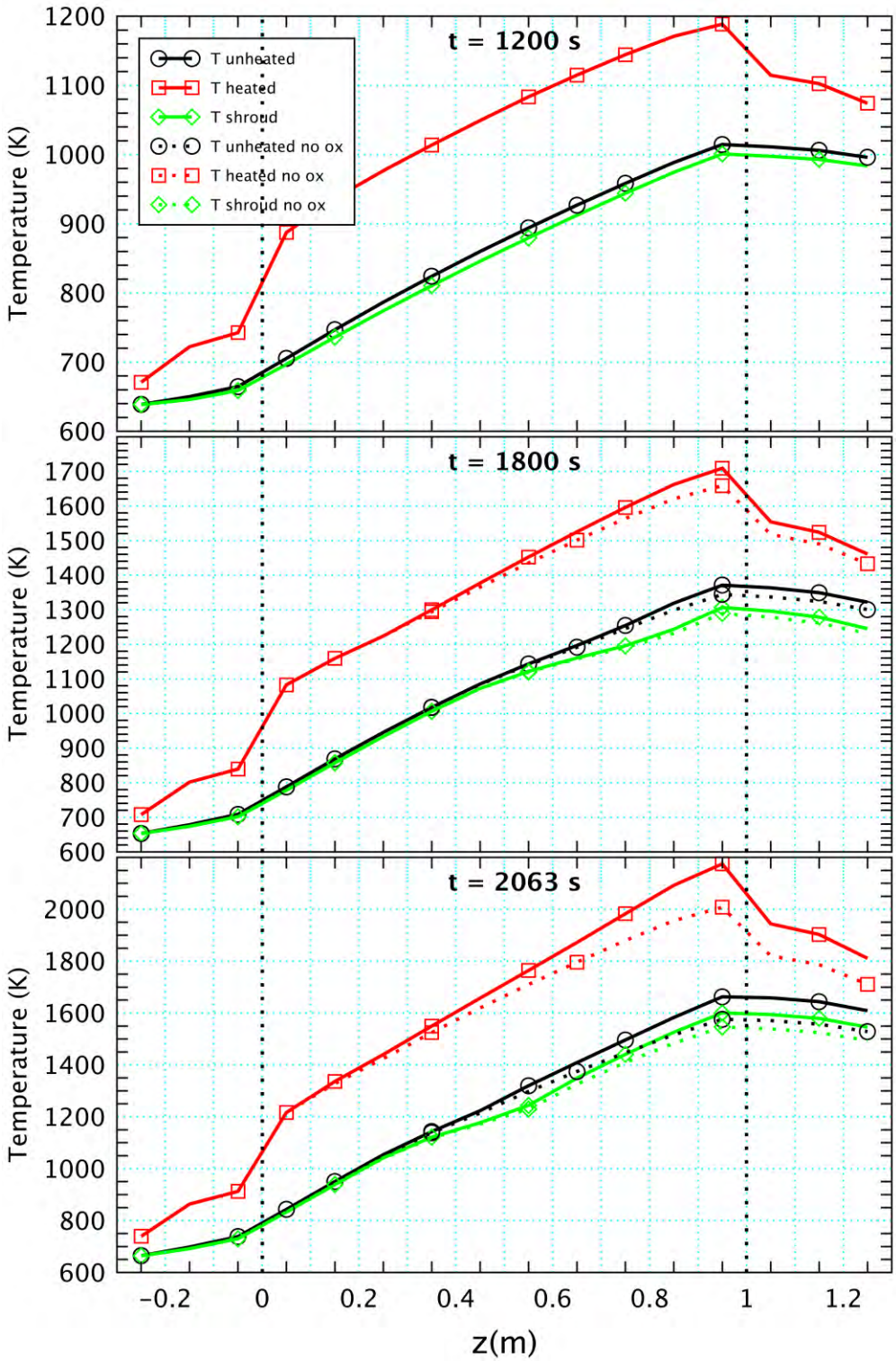

Figure 26 Axial profiles for cases A and C with TRACE
The figure shows axial temperature profiles of the central rod, the inner heated rods, and the shroud at various times.

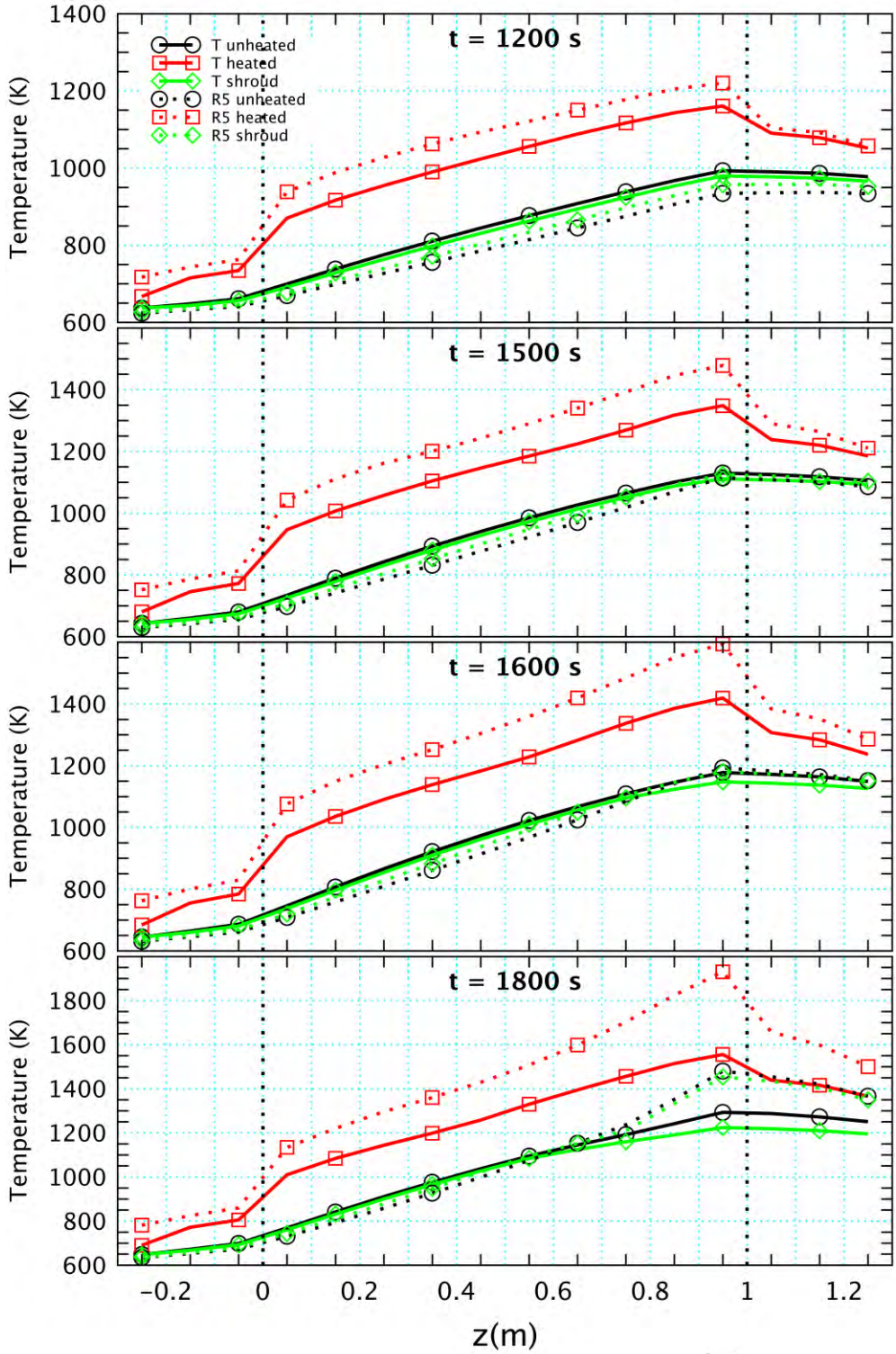

Figure 27 Axial profiles for case B with TRACE and R5
The figure shows axial temperature profiles of the central rod, the inner heated rods, and the shroud at various times.

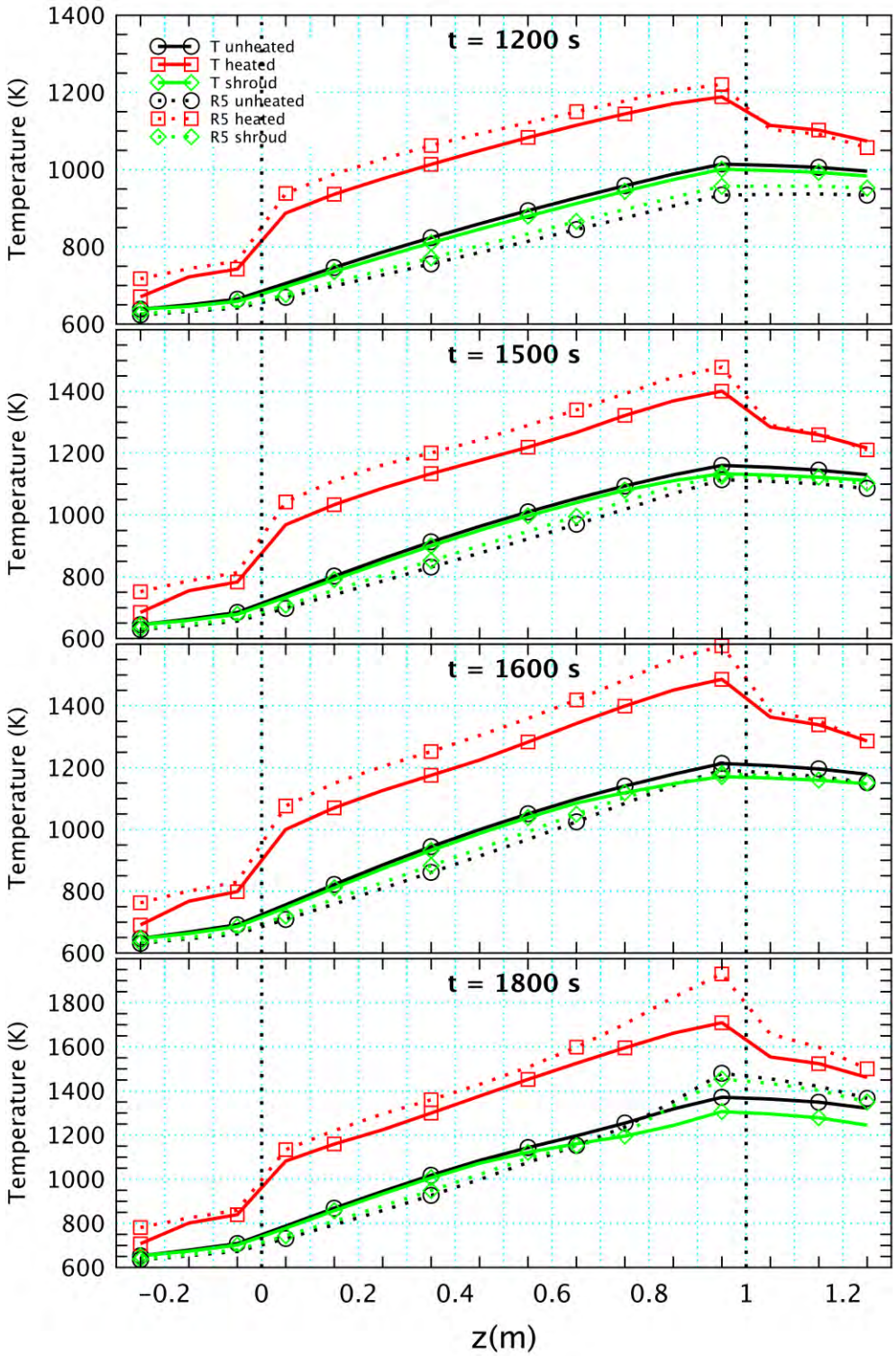

Figure 28 Axial profiles for case C with TRACE and R5

The figure shows axial temperature profiles of the central rod, the inner heated rods, and the shroud at various times.

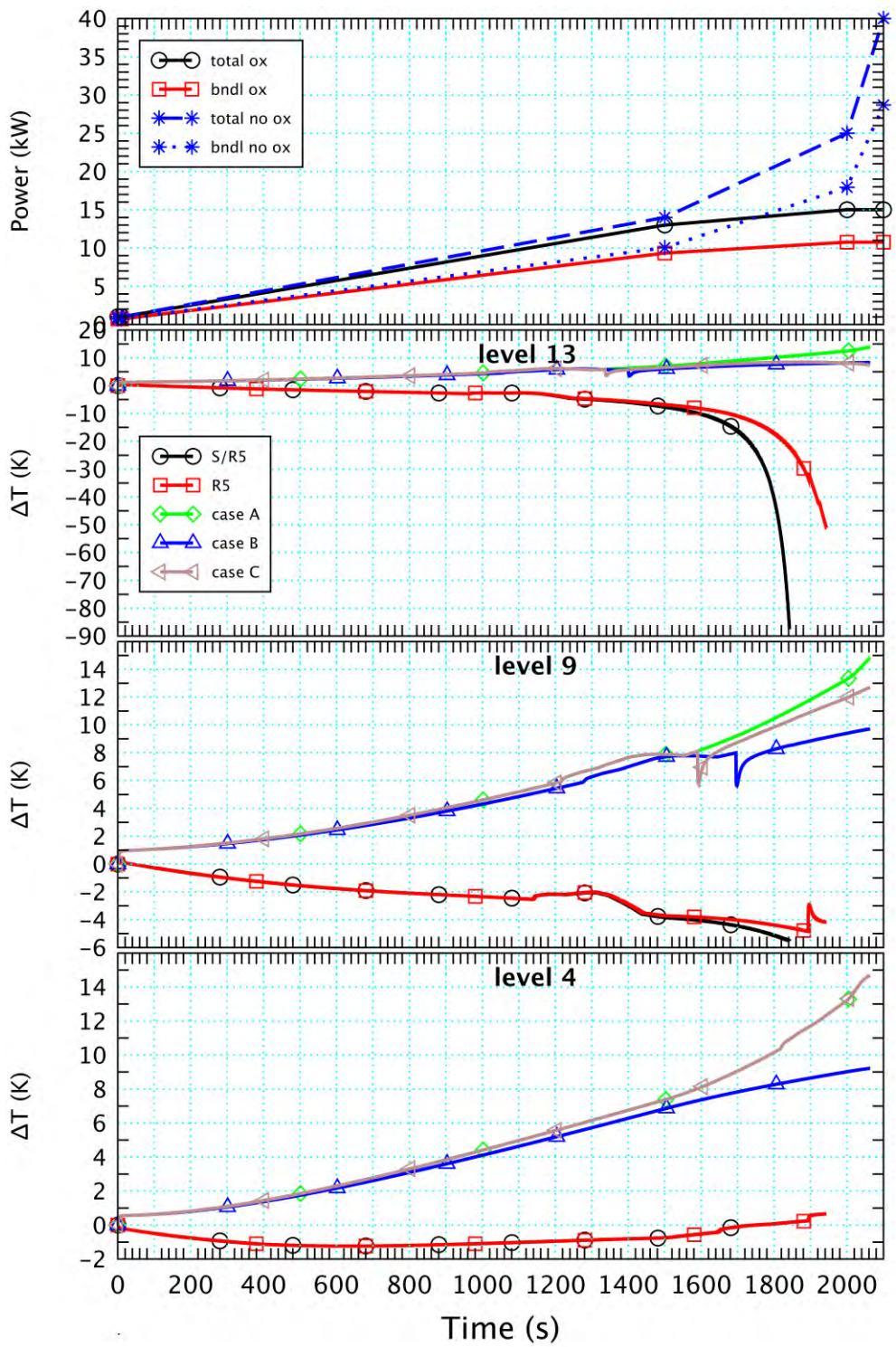

Figure 29 Radial rod temperature differences at various axial levels
The graph shows the difference between centerline and outer clad surface temperatures for heated rods for SCDAP/RELAP5 and RELAP5 with oxidation and for the three cases for TRACE.

7 CONCLUSIONS

To assess the code capabilities of RELAP5 and TRACE for delayed reflood situations, the conditions before reflood initiation were considered as a first step. The steam cool-down test QUENCH-04, performed at the former Forschungszentrum Karlsruhe, now part of the Karlsruhe Institute of Technology (KIT), and related post-test calculations with SCDAP/RELAP5 (S/R5) proved to be an appropriate basis. The experimental basis guarantees that the chosen computational case is prototypical for reflood scenarios. Though the post-test calculations might be improved, the deviations from experimental results are no serious problem in the context of the present investigations. In this way, the work could be done as a combination of a code-to-code comparison and a comparison of calculated with experimental results. The strategy to use S/R5, RELAP5, and TRACE in that sequence proved to be useful, taking the existing input deck for S/R5 as a basis.

Application of S/R5 for QUENCH-04 demonstrated that for the chosen scenario sensible oxidation effects are restricted to the hot zone, but that they cannot be neglected above about 1200 K, i.e. in a temperature region, where RELAP5 and TRACE can still be used. This result shows the importance of an appropriate oxidation model in such codes.

The RELAP5 oxidation model cannot be activated for a shroud. This shortcoming has the consequence that as much as 25 % of the total oxidizing surface is not considered in the present calculations. In addition, the application of RELAP5 to QUENCH-04 revealed a severe error during program execution, leading to an abnormal end of the calculation.

Subsequent simplifications and modifications of the original input deck for the QUENCH test led to the consideration of an artificial alternate bundle for further calculations. When the oxidation mode is deactivated, nearly the same temperatures are calculated with RELAP5 and S/R5. The abnormal end of the RELAP5 calculations for QUENCH-04 was seen to be related to the oxidation model or its implementation in the code, but that it is not correlated directly with temperature.

Calculations with TRACE showed far smaller temperature increases than expected, when the oxidation model is activated, suggesting that the release of chemical power is not calculated correctly. During the conversion of the RELAP5 input deck for TRACE with SNAP, shortcomings of this conversion tool were detected that should be removed.

In sum, both codes RELAP5 and TRACE show severe, but different problems concerning oxidation, when they are applied to the heat-up phase of a prototypical reflood scenario. Since the related effects cannot be neglected at higher temperatures, these code errors should be corrected. If this work cannot be done, the use of these codes should be restricted to temperatures, where oxidation is negligible. In addition, some plot capabilities of both RELAP5 and TRACE are inferior to those of S/R5 and should be adapted from that code.

A complete comparison of the various codes has also to consider the reflood phase itself, but this can only be done, when the code errors, addressed above, are removed. In test QUENCH-11 [15], the whole accident sequence from boil-off to reflood was simulated. In pre-test QUENCH-11v3, this test sequence was applied, but maximum heat-up temperature was restricted to about 1350 K. Since data acquisition of the pre-test comprises all variables that are considered in the main test and since the whole test is within the application range of RELAP5

and TRACE, especially concerning the maximum temperature, this pre-test is an excellent basis for such investigations.

8 REFERENCES

[1] Information Systems Laboratories, Inc. Rockville, Maryland, Idaho Falls, Idaho, USA: RELAP5/MOD3.3 Code Manual, NUREG/CR-5535/Rev P3-Vol I, March 2003.

[2] U. S. Nuclear Regulatory Commission: TRACE V5.0, Washington, DC, USA, October 2008.

[3] Idaho National Engineering and Environmental Laboratory, Lockheed Martin Idaho Technologies, Idaho Falls, Idaho 83415, USA: SCDAP/RELAP5/MOD3.2 Code Manual, NUREG/CR-6150, INEL-96/0422, October 1997.

[4] Projekt Nukleare Sicherheitsforschung / Jahresbericht 1996, p. 351-352, Forschungszentrum Karlsruhe, FZKA 5963, September 1997.

[5] Hering, W., Homann, Ch.: Improvement of the SCDAP/RELAP5 code with respect to FZK experimental facilities. Forschungszentrum Karlsruhe, FZKA-6566, June 2007.

[6] Sepold, L., Hofmann, P., Homann, C., Leiling, W., Miassoedov, A., Piel, D., Schanz, G., Schmidt, L., Stegmaier, U., Steinbrück, M., Steiner, H., Palagin, A.V., Boldyrev, A.V., Berdyshev, A.V., Shestak, V.E., Veshchunov, M.S.: Investigation of an overheated PWR-type fuel rod simulator bundle cooled down by steam. Part I: Experimental and calculational results of the QUENCH-04 test. Part II: Application of the SVECHA/QUENCH code to the analysis of the QUENCH-01 and QUENCH-04 bundle tests. Forschungszentrum Karlsruhe, FZKA-6412, April 2002.

[7] Applied Programming Technology, Inc., Bloomsburg PA, USA: Symbolic Nuclear Analysis Package (SNAP) User's Manual, November 2006.

[8] Steinbrück, M.: Analysis of Hydrogen Production in QUENCH Bundle Tests. Forschungszentrum Karlsruhe, FZKA 6968, May 2004.

[9] Sanchez, V., Elias, E., Homann, Ch., Hering, W., Struwe, D.: Development and Validation of a Transition Boiling Model for the RELAP5/MOD3 Reflood Simulation. Forschungszentrum Karlsruhe, FZKA 5954, September 1997.

[10] Hofmann, P., Hering, W., Homann, C., Leiling, W., Miassoedov, A., Piel, D., Schmidt, L., Sepold, L.; Steinbrück, M.: QUENCH-01 Experimental and Calculational Results. Forschungszentrum Karlsruhe, FZKA 6100, November 1998.

[11] Schanz, G.: Recommendations and supporting information on the choice of zirconium oxidation models in severe accident codes. Forschungszentrum Karlsruhe, FZKA-6827, March 2003, SAM-COLOSS-P043.

[12] Steinbrück, M., Miassoedov, A., Schanz, G., Sepold, L., Stegmaier, U., Steiner, H., Stuckert, J.: Results of the QUENCH-09 experiment with a B_4C control rod. Forschungszentrum Karlsruhe, FZKA-6829, December 2004.

[13] Hofmann, P., Homann, C., Leiling, W., Miassoedov, A., Piel, D., Schmidt, L., Sepold, L.; Steinbrück, M.: Results of the QUENCH commissioning tests. Forschungszentrum Karlsruhe, FZKA-6099, August 1998.

[14] Chris Murray, US NRC, private communication at CAMP-2010 Spring Meeting, June 9 – 11, 2010, Stockholm, Sweden.

[15] Hering, W., Groudev, P., Heck, M., Homann, C., Schanz, G., Sepold, L., Stefanova, A., Stegmaier, U., Steinbrück, M., Steiner, H., Stuckert, J.: Results of Boil-Off Experiment QUENCH-11. Forschungszentrum Karlsruhe, FZKA-7247, SAM-LACOMERA-D18, June 2007.

APPENDIX A OXIDATION MODELS

In all three codes, SCDAP/RELAP5, RELAP5, and TRACE models for oxidation of Zircaloy are available, but in different ways. As a common feature, parabolic rate equations are considered for oxidation.

In SCDAP/RELAP5, this is done for the weight gain as well as for the thickness of the oxide layer and the a-Zr(O) layer. Oxidation starts at 923 K. The change of oxidation kinetics at about 1850 K is considered by changing the rate constants according to open literature. The hydrogen production rate is calculated directly from the weight gain; chemical heat generation is calculated directly from the hydrogen production rate. The hydrogen release is considered as non-condensable in the basic fluid equations; the amount of consumed steam is also considered.

When steam supply is insufficient, oxidation is limited on the basis of an analogy for mass and heat transfer. Oxidation is terminated, when the Zircaloy material is entirely converted into ZrO_2. For ruptured claddings, oxidation of the inner clad surface is assumed to occur with the same rate as for the outer clad surface. Special cases like the oxidation of Zircaloy on debris are considered separately.

In RELAP5, the parabolic rate equation is solved for the oxide layer thickness. This value is used to derive the cumulated hydrogen mass. The released chemical power is calculated from the increase of oxide layer thickness. Oxidation of the inner surface of ruptured claddings is taken into account. Oxidation is terminated, when the whole amount of available Zircaloy is consumed. Thermal-physical properties of the cladding are not changed; neither hydrogen release nor steam consumption considered in the basic fluid equations.

In TRACE, the parabolic rate equation is applied to oxygen consumption, if the rod temperature exceeds 1273 K. The result is converted to the thickness an effective ZrO_2 layer, using an approximation of the respective densities. The release of chemical heat is computed from the increase of oxide layer thickness.